Published in final edited form as:

EcoSal Plus. 2009 August ; 3(2): . doi:10.1128/ecosalplus.3.6.1.9.

Biosynthesis of Histidine

MALCOLM E. WINKLER[*] and **SMIRLA RAMOS-MONTAÑEZ**

Department of Biology, Indiana University Bloomington, Bloomington, IN 47405

INTRODUCTION

The biosynthesis of histidine in *Salmonella typhimurium* (official designation, *Salmonella enterica* serovar Typhimurium) and *Escherichia coli* has been an important system for the study of relationships between the flow of intermediates through a biosynthetic pathway and the control of the genes encoding the enzymes that catalyze the steps in the pathway. Earlier studies of histidine biosynthesis contributed to understanding mechanisms basic to the regulation of biosynthetic pathways, such as feedback inhibition, energy charge, and the setting of basal biosynthetic enzyme levels. The histidine biosynthetic pathway itself contains several interesting and unusual intermediates and enzymatic steps and forms a critical link between amino acid, purine, and thiamine biosynthesis. Fundamental concepts in gene regulation, such as attenuation, Rho factor-dependent polarity, the polycistronic organization of mRNA molecules, autogenous regulation, transcriptional pausing, and positive control of metabolic regulation, were formulated to explain aspects of histidine biosynthesis. In fact, the term “attenuation” was first coined to describe regulatory patterns of the histidine operon (132). In addition, the histidine biosynthetic pathway and the histidine operon have served as a powerful model system for studying fundamental evolutionary, metabolic, physiological, and genetic processes, such as gene duplications, transposition, mutagenesis, including the widely used Ames test (13, 101), and tRNA biosynthesis and function.

The first comprehensive review of histidine biosynthesis was written by Brenner and B. N. Ames in 1971 (42). This extraordinary article consolidated information about control of the histidine biosynthetic pathway and posed many of the questions about histidine biosynthesis and *his* operon control that were the subject of investigation in subsequent years. Later reviews, including the first two versions of this review in 1987 and 1996, and reviews by Blasi and Bruni (34) and Artz and Holzschu (25), covered the developments of the molecular structure of the *his* operon, the mechanisms of *his* operon metabolic regulation and attenuation control, and the function of the *his* regulatory loci, including identification of *hisW* mutations and one class of *hisU* mutations as alleles of *gyrA* and *gyrB*, respectively, which encode the subunits of DNA gyrase. The 1996 review by Alifano *et al.* (4) is noteworthy and describes histidine biosynthesis in organisms besides *E. coli* and *S. typhimurium* and provides one of the first summaries of the evolution of the histidine biosynthetic pathway.

[*]Corresponding author. Mailing address: Department of Biology, Indiana University Bloomington, Jordan Hall, Room 142, Bloomington, IN 47405. Phone: (812) 856-1318. mwinkler@bio.indiana.edu..

Since the previous version of this review, exceptional progress has been made in a couple of research areas. Most of the enzymes that catalyze histidine biosynthesis have now been crystallized and had their structures determined. Many of the histidine biosynthetic intermediates are unstable, and the histidine biosynthetic enzymes catalyze some chemically unusual reactions. Therefore, these studies have led to considerable mechanistic insight into the pathway itself and have provided deep biochemical understanding of several fundamental processes, such as feedback control, allosteric interactions, and metabolite channeling. Highlights from these studies are summarized in this review. At the same time, some of the older physiological information from the previous versions of this review has been retained and updated because of its metabolic importance and use in understanding *his* operon control. One particularly satisfying generalization that can be drawn from the recent biochemical work is just how accurate the older results and models turned out to be, especially given the relative limitations of the methods then available. Considerable recent progress has also been made on aspects of *his* operon regulation, including the mechanism of pp(p)Gpp stimulation of *his* operon transcription, the molecular basis for transcriptional pausing and Rho factor-mediated polarity. These and other developments are summarized. The large number of genomic sequences that continue to be determined has sustained interest in the evolution of the histidine biosynthetic pathway and enzymes in eubacteria, archaea, fungi, and plants. Evolution is touched upon in this review as it relates to *E. coli* and *S. typhimurium*. Several additional reviews on the evolution of histidine biosynthesis in different organisms, including plants, have recently appeared (4, 85-87, 162, 179, 204).

THE HISTIDINE BIOSYNTHETIC PATHWAY AND ENZYMES

Intermediates in the Pathway

The pathway and details of histidine biosynthesis are the same in *E. coli* and *S. typhimurium* (34). In fact, the same pathway is used in all organisms that synthesize histidine, although there are variations in the genetic organization and grouping of the biosynthetic enzymes (4, 162, 166, 203, 204). Histidine has been postulated to have formed abiotically, and histidine-containing peptides may have been involved in the prebiotic synthesis of peptides and nucleic acid molecules (see (4, 85)). Analyses of the distribution of the histidine biosynthesis genes suggest that a series of duplication, elongation, and fusion events were involved in the evolution of this biologically ancient pathway (4, 179). The ten biochemical steps in this unbranched pathway include a number of complex and unusual reactions, and all nine chemical intermediates have been described chemically (Fig. 1). A new method to determine metabolome changes based on tandem capillary electrophoresis and mass spectrometry has shown that these intermediates accumulate rapidly in an *E. coli hisD* mutant abruptly starved for histidine (171). This starvation condition also induces the stringent response, which leads to increases in the levels of ppGpp, ATP, GTP, amino acids and changes in intermediates in pathways subjected to stringent control (171).

The determination of the pathway was started by the work of B. N. Ames and coworkers (see references in (42)) and completed only recently by Klem and Davisson (137). For simplicity, the eight enzymes that catalyze the reactions (Table 1) are designated by the genes that encode them in the *his* operon. Three of the proteins, HisI, HisB, and HisD, are

bifunctional in *E. coli* and *S. typhimurium* and carry out two separate reactions in the pathway (Table 1 and Fig. 1). Two other proteins, HisH and HisF, form an obligate heterodimer (Table 1). Phosphoribosylpyrophosphate (PRPP) and ATP are the initial substrates and connect histidine biosynthesis with the biosynthesis of pyrimidine nucleotides, purine nucleotides, pyridine nucleotides, thiamine, and tryptophan (see chapters XX, XX, XX, and XX, respectively, in this volume). The metabolic link between histidine and purine biosynthesis is indicated by numerous observations. For example, *S. typhimurium* mutants that have increased expression of the *his* operon and lack feedback control of the histidine biosynthetic pathway require adenine for growth at 42°C (128). Histidine starvation of *hisF* mutants, which cannot recycle 5-aminoimidazole-4-carboxamide ribonucleotide (AICAR) for purine biosynthesis (Fig. 1), results in a 15-fold drop in cellular ATP pools without severely lowering GTP, UTP, and CTP levels (125). This observation forms the basis of a reversible method to deplete cellular ATP pools to around 100 μM (125). Along the same line, *E. coli* strains carrying leaky frameshift mutations in the promoter-distal part of *hisH* grow when supplemented with purines, such as inosine, without histidine (178). These leaky *hisH* mutants also grow on medium lacking purines or histidine when the histidine biosynthetic pathway is partially feedback inhibited by a histidine analog (see below). All these observations can be explained by futile ATP consumption by the first part of the histidine biosynthetic pathway without recycling of the purine precursor, AICAR (Fig. 1). In addition, recent work has shown that metabolic flux in the purine and histidine biosynthetic pathways can influence the synthesis of thiamine, whose synthesis branches from the purine pathway (9). The requirement of *S. typhimurium purH* mutants for thiamine can be satisfied by histidine in a parent strain, but not in a mutant lacking feedback control. This result can be explained by a model in which AICAR accumulation by the *purH* mutant blocks thiamine biosynthesis, and histidine addition reduces the flux through the histidine pathway, reduces AICAR amount, and relieves the inhibition on thiamine biosynthesis (9).

The first reaction in the pathway is catalyzed by the HisG protein and involves a displacement on C-1 of PRPP by N-1 of the purine ring of ATP (Fig. 1). This Mg^{+2} ion-dependent condensation releases a pyrophosphate molecule, inverts the ribose moiety derived from PRPP from the α to the β configuration, and although reversible, is strongly product inhibited by L-histidine. The role played by feedback inhibition of the HisG enzyme in controlling the flow of intermediates through the histidine pathway is discussed in another section. Recent genome-scale metabolic modeling of *E. coli* indicates that this first reaction in histidine biosynthesis is one of the rare (5 of 873) thermodynamically unfavorable reactions involved in biomass production (114). The conclusion suggests that product inhibition likely limits flux into the histidine pathway (below and (114)).

The next steps in the pathway involve irreversible, Mg^{+2} ion-dependent hydrolysis of the N ′-5-phosphoribosyl-ATP to N′-5′-phosphoribosyl-AMP and pyrophosphate catalyzed by the carboxyl terminal domain of the HisI enzyme, followed by a ring-opening reaction catalyzed by the amino terminal domain of HisI (Fig. 1). An internal redox reaction, known as an Amadori rearrangement, follows and is catalyzed by the HisA gene product (Fig. 1). For some time, the order and number of the next biosynthetic steps were not unequivocally established, and it was thought that at least one intermediate of unknown structure existed

(201). However, it is now established from biochemical and structural characterization (10, 11, 136, 137, 164, 165) and the phenotypes of *hisH* and *hisF* mutants (125, 128, 178) that HisH and HisF are subunits of a single imidazoleglycerol phosphate (IGP) synthase that produces IGP and AICAR directly. Besides being cycled back to purine biosynthesis, AICAR is a precursor of the unusual ribotriphosphate 5-amino-4-imidazole carboxamide riboside 5′-triphosphate (ZTP in Fig. 1) (36). For this and other reasons, mutation frequencies were measured in *E. coli* with altered AICAR pools; however, AICAR was found not to be an endogenous metabolic mutagen (93, 95).

The final steps in histidine biosynthesis include a Mn^{+2} ion-dependent dehydration catalyzed by the carboxyl terminal domain of the HisB protein followed by a ketonization of the resulting enol, a reversible transamination with a nitrogen atom from glutamate catalyzed by the pyridoxal 5′- phosphate-containing HisC enzyme, and a dephosphorylation of L-histidinol phosphate catalyzed by the amino terminal domain of HisB. The L-histidinol product is then converted via an unstable histidinaldehyde intermediate to histidine by the bifunctional Zn^{+2}-ion dependent HisD dehydrogenase (26, 108). This conversion involves two consecutive oxidation steps linked to the reduction of two NAD^+ molecules (26, 108). In summary, the atoms of histidine are derived from the following precursors through the biosynthetic pathway: three carbon atoms of the amino acid backbone and carbons 4 and 5 of the imidazole ring are from PRPP, the amino group is from glutamate, nitrogen 3 of the imidazole ring is from glutamine, and carbon 2 and nitrogen 1 of the imidazole ring are from ATP.

Regulation of the Pathway

Energy equivalent to about 41 ATP molecules is required to synthesize each histidine molecule (42). Consequently, a bacterium that completely lacks control of histidine biosynthesis will waste about 2.5% of its metabolic energy synthesizing excess histidine when growing with a doubling time of about 50 min (42). For this reason, it is not surprising that *E. coli* and *S. typhimurium* have evolved an elaborate network to control the rate of histidine biosynthesis. The two most important points of control are regulation of the flow of intermediates through the pathway and regulation of the amounts of histidine biosynthetic enzymes produced.

Regulation of the Flow of Intermediates through the Pathway—The flow of intermediates through the histidine biosynthetic pathway can be adjusted by varying the enzymatic activity of the HisG enzyme, which catalyzes the first reaction in the pathway (Fig. 1). Modulation of HisG enzyme activity is brought about by four interrelated forms of inhibition: (i) classical, noncompetitive feedback inhibition by histidine; (ii) inhibition by ppGpp in the presence of partially inhibiting concentrations of histidine; (iii) competitive inhibition by ADP and AMP in response to the overall energy status in the cell; and (iv) competitive product inhibition by phosphoribosyl-ATP (PR-ATP) (Fig. 1). In wild-type bacteria growing in minimal medium, the rate of histidine biosynthesis seems to be controlled primarily by regulation of HisG enzymatic activity. Several feedback-resistant and feedback-hypersensitive mutations were mapped in a region that encodes the carboxyl-terminal portion of the HisG protein (119, 206). Feedback-resistant mutants selected for

their growth in the presence of the analog 2-thiazolealanine excrete histidine into the culture medium (194). This important observation indicates that feedback inhibition holds histidine biosynthesis far below its full capacity, even when histidine is not supplied as a supplement (42). Some feedback-hypersensitive mutants also have a distinct phenotype; they are growth restricted at 20°C because of severe inhibition of the mutant HisG enzyme by histidine at lower temperatures (170, 206).

Because of its crucial role, the enzymology of the HisG protein has been intensively studied (Table 1). One potential problem in interpreting HisG kinetic data is strong product inhibition by phosphoribosyl-ATP (PR-ATP) (Fig. 1) (71, 208). To minimize this product inhibition, HisG enzyme assays were coupled to HisI activity to convert PR-ATP to the next intermediate in the pathway (208). Stopped-flow kinetic analyses of the HisG reaction have also been performed (71). Another earlier issue about HisG enzymology was the aggregation state of the protein, which was influenced in a complex way by temperature, ionic strength, pH, and the presence of ligands and effectors (34, 71). The combined kinetic studies have led to the following picture of the regulation of HisG activity. (i) Active HisG is a dimer that is stabilized by the substrate PRPP (208, 209); (ii) HisG dimers are in equilibrium with an inactive hexamer form whose formation is favored by binding the PR-ATP product, AMP, ADP, or histidine (140, 208); (iii) AMP and ADP are competitive inhibitors for both of the substrates, PRPP and ATP (160), whereas histidine acts through an allosteric mechanism that does not overlap the enzyme active site (159); (iv) inhibition by AMP and histidine is synergistic (71), and histidine causes discrimination against ATP binding in favor of the co-inhibitors, AMP and ADP (160).

The apparent K_m of the HisG enzyme for ATP is much lower than the intracellular ATP concentration, whereas the apparent K_m for PRPP is probably closer to the intracellular PRPP concentration (Table 1 and footnote a to Table 2); therefore, the rate of histidine biosynthesis most likely is directly affected by variations in the intracellular PRPP pool size. Since ATP and PRPP are the first substrates in the pathway and considerable cellular energy is consumed in histidine biosynthesis, inhibition of HisG enzyme activity by AMP and ADP has frequently been cited as an example of an energy-utilizing system that responds to the overall energy status in the cell, as expressed by the Atkinson energy-charge formula (42, 138). The K_i of the HisG enzyme for histidine (Table 1) is comparable to the intracellular histidine concentration found in bacteria growing in minimal medium containing histidine (Table 2), an observation that implies substantial inhibition of the rate of biosynthesis through the pathway. In contrast, the K_i for histidine is considerably higher than the intracellular histidine concentration found in bacteria that must synthesize histidine.

Three recent structural studies have provided the first insights into the mechanism of HisG allosteric control (56, 65, 150). The structure of HisG from *Mycobacterium tuberculosis* was determined without bound ligand and complexed with inhibitors AMP and histidine (65). The structure of HisG from *E. coli* was determined complexed with the inhibitor AMP or the PR-ATP product (150). Last, the structure of the HisG-HisZ complex from *Lactococcus lactis* was determined complexed with the substrate PRPP or with phosphate ion and ATP (56). From these combined crystal structures and previous biochemical studies (Table 1 and above), the following picture of HisG feedback control emerges. (i) The Mg^+-dependent

HisG ATP-phosphoribosyltransferase (ATP-PRTase) reaction proceeds by an ordered Bi-Bi kinetic mechanism by which ATP binds before PRPP and PPi leaves before PR-ARP (see (150)). (ii) HisG ATP-PRTases represent a separate class of PRTs, designated as type IV, that have a fold related to that in periplasmic binding proteins (56, 65, 150). Lack of amino acid sequence similarity and the differences in structure suggests that the different types of PRTs arose by convergent evolution (150). (iii) Each monomer of HisG consists of three domains; domains I and II form a crevice used as the catalytic core, and the carboxyl terminal domain III binds to histidine (56, 65, 150). (iv) ATP and PRPP substrate binding favors dimer formation and causes the enzyme to assume an activated state similar to that of glycosyltransferases (56, 150). This state involves a conformational change at the dimer interface that brings into the active site conserved amino acids that promote pyrophosphate group leaving (56) (v) The "long" form of HisG found in *E. coli*, *S. typhimurium*, *M. tuberculosis*, and related bacteria has a fundamentally different quaternary structure (dimers and hexamers) from that of the *L. lactis* "short" form of HisG (heterooctamer). The catalytic HisG subunit of the short form is missing about 100 amino acids from its carboxyl terminus compared to the long form and requires heterodimer formation with a separate HisZ subunit for activity (56, 198). The HisZ subunit is a paralog of amino acyl-tRNA synthetases (198), although it lacks this activity. The remaining properties of HisG allosteric control discussed here refer to the long form found in *E. coli* and *S. typhimurium.* Further information about the HisZ subunit is in references (39, 198), and the structures of the HisG short and long forms are compared in reference (56)

(vi) Competitive inhibition of ATP and PRPP binding by AMP is caused by binding of a monophosphate and the ribose ring of AMP to the PRPP binding site in domain II and binding of the adenine ring of AMP to the ATP binding site in domain I (150). In addition, AMP and the product PR-ATP cause the catalytically active ATP-PRT dimers to aggregate into inactive hexamers, which are formed by binding together the carboxyl terminal ends of three dimers (65, 150). Aggregation into hexamers structurally closes the active site of the enzyme (65, 150). (vii) Binding of AMP and histidine induces a large conformational change in HisG that causes steric hindrance of the active sites in domains I and II (65). Binding of AMP orients residues in the carboxyl terminal domains of the hexamer subunits and thereby increases the affinity for histidine (65, 150) Conversely, the conformation change that occurs upon histidine binding decreases the dissociation of AMP from the active site.

The basis for inhibition of HisG by the alarmone ppGpp awaits future structural elucidation. ppGpp, which is a positive effector of *his* operon transcription (see below), does not inhibit HisG enzyme activity by itself; however, in the presence of moderate histidine concentrations (≥25 μM), physiologically significant concentrations of ppGpp (≥200 μM) strongly inhibit HisG enzyme activity in a positively cooperative manner (161). The synergistic inhibition of HisG enzyme by ppGpp and histidine might play a physiological role (25). Starvation of bacteria for amino acids elicits ppGpp accumulation as part of the stringent response (see Chapter XX). If bacteria are starved for an amino acid in the presence of histidine, then the synergistic inhibition of HisG enzyme by intracellular ppGpp (≥200 μM) and histidine (≈100 μM) will completely inhibit histidine biosynthesis. In

contrast, ppGpp accumulation in bacteria starved for histidine will not inhibit the HisG enzyme. In addition, HisG enzyme activity will not be strongly inhibited by the intracellular pools of histidine (≈15 μM) and ppGpp (≈30 μM) present in bacteria growing exponentially in minimal medium lacking histidine.

In summary, the HisG ATP-PRTase is a complicated protein that is present in multiple aggregation states in response to its substrate and combinations of the inhibitors histidine, ppGpp, AMP, ADP, and PR-ATP. This multivalent inhibition allows sensitive control of the rate of histidine biosynthesis in response to a variety of cellular metabolic states. This complex, multivalent control is required because histidine biosynthesis is regulated chiefly by modulating the flow of intermediates through the pathway in wild-type bacteria growing under common culture conditions, as discussed in the next section. Recent structural studies can account for most of the catalytic, inhibition, and aggregation properties of the HisG ATP-PRTase. This combination of biochemical and structural information provides powerful information about the mechanism of allosteric feedback inhibition of the critical HisG enzyme.

Regulation of the Amounts of Histidine Biosynthetic Enzymes—In effect, noncompetitive inhibition by histidine lowers the apparent V_{max} of the HisG enzyme reaction and makes it appear as if less total enzyme were present (152). Another way to control the rate of histidine biosynthesis is to adjust the intracellular concentrations of the histidine biosynthetic enzymes in response to histidine and other metabolites. The structure and regulation of the *his* operon, which encodes all of the histidine biosynthetic enzymes (Fig. 2 and Table 3), have been subjects of investigation for over fifty years. Results from many studies show that two mechanisms regulate *his* operon expression at the level of transcription: (i) transcription initiation at the *his* operon primary promoter (*hisp1*) is positively regulated by increasing ppGpp concentrations up to the ppGpp concentration found in cells growing in minimal-glucose medium; and (ii) transcription of the *his* structural genes is regulated by an attenuation mechanism that responds to the intracellular concentration of His-$tRNA^{His}$. The concentration of His-$tRNA^{His}$ is, in turn, determined by cellular histidine concentration, histidyl-tRNA synthetase activity and amount, and chromosomal DNA supercoiling levels in response to anaerobiosis and osmolarity (Tables 2 and 3; see below).

When *E. coli* and *S. typhimurium* are growing in a nutrient-rich medium, there apparently is an advantage in decreasing the amounts of the histidine biosynthetic enzymes by about four fold (Table 2). This metabolic regulation, which gears histidine biosynthesis to cellular growth rate, appears to be mediated by ppGpp and is independent of His-$tRNA^{His}$-specific attenuation control (see below) (184, 193, 205, 223). Surprisingly, *in vivo his* operon expression is largely unaffected by the presence of histidine in the growth medium (Table 2), despite the potential for a wide range of control by His-$tRNA^{His}$-specific attenuation. This unusual feature of *his* operon expression partly reflects the fact that histidine addition does not greatly increase the percentage of $tRNA^{His}$ molecules charged with histidine (Table 2). Consequently, even when exogenous histidine is absent from growth media, the amount of charged $tRNA^{His}$is still relatively high. Another surprising feature of his operon attenuation is that even when 77 to 88% of $tRNA^{His}$ molecules are charged with histidine,

there is significant readthrough transcription beyond the *his* attenuator. The high basal level of wild-type *his* operon expression is most readily apparent in bacteria containing mutations that increase *his* operon attenuation. These mutations, which prevent translation of the *his* leader peptide or formation of the antiterminator RNA secondary structure (see below), completely prevent transcription of the *his* operon structural genes and cause histidine auxotrophy (126, 127). Clearly, there is a much greater potential to limit *his* operon expression by attenuation than is actually used in the bacterium growing under the laboratory conditions tested so far. A mechanism that might contribute to setting the basal level of his attenuation is described in the section on regulation of the *his* operon. The need to maintain relatively high cellular concentrations of the histidine biosynthetic enzymes may be related to the high affinity of the histidine periplasmic transport system and is discussed near the end of this review.

The attenuation mechanism also modulates *his* operon expression in response to physiological conditions that change chromosomal DNA supercoiling density, such as anaerobiosis and osmolarity (169). *his* operon expression is found to increase when the bacterial chromosome relaxes (i.e., is less negatively supercoiled), as occurs in DNA gyrase mutants or in wild-type bacteria during growth in the presence of oxygen and low osmolarity or upon addition of DNA gyrase inhibitors, such as novobiocin (169). For example, in stationary-phase cells, novobiocin addition increases *his* operon expression about 10-fold, and this effect is reversed by salt addition or anaerobiosis. Even without novobiocin addition, *his* operon expression is reduced by high osmolarity or anaerobiosis (169). This experimental result does not support a prediction from a recent metabolic network model that *his* operon expression should increase during oxygen deprivation (190). Other experiments with mutants lacking the *his* attenuator region (Δ*his01242*) or defective in ppGpp synthesis (*relA*) indicated that supercoiling control of his operon expression occurs mostly by changes in attenuation rather than by changes in the frequency of transcription initiation from the primary promoter *hisp1* (see below). Several lines of investigation support the idea that supercoiling control of *his* operon attenuation is mediated by changes in the total cellular content of $tRNA^{His}$ molecules, encoded by the HisR gene (90, 169, 187). The regulation of *hisR* by DNA supercoiling and the identification of the early *his* regulatory loci, *hisW* and *hisU(I),* as mutant alleles of *gyrA* and *gyrB*, respectively, are considered later in this review.

The Histidine Biosynthetic Enzymes

Since the last version of this review, there has been an explosion of knowledge about the structure and biochemical mechanisms of most of the histidine biosynthetic enzymes. Table 1 compiles these recent references and some of the older ones whose results have held up well over time. The biochemistry and structural basis for allosteric feedback inhibition of the HisG ATP-PRTase is presented above. In this section, I briefly summarize some of the most important conclusions about the other histidine biosynthetic enzymes from these recent structure and mechanism papers. Where possible, I focus the scope of this section on enzymes from *E. coli* and *S. typhimurium.* Some definitive structural and biochemical papers using enzymes from thermo-stable prokaryotes are discussed for enzymes that have proven

difficult in the enteric bacteria. The references cited and the NCBI Entrez site should be consulted for the structures and additional details.

Bifunctional HisI—The carboxyl and amino terminal domains of the HisI enzyme catalyze the second PR-ATP pyrophosphohydrolase (sometimes called HisE) and third PR-AMP-cyclohydrolase steps, respectively, of histidine biosynthesis (Fig. 1 and above). Bifunctional HisI has been biochemically intractable (69). The protein tends to be unstable and has ill-defined metal coenzyme requirements. For this reason, the monofunctional PR-AMP-cyclohydrolase from *Methanococcus vannielii* was characterized biochemically (69), and the structure of HisI from *Methanobacterium thermoautotrophicum* was determined (200). The PR-ATP pyrophosphohydrolase (step 2) remains the only enzyme in the histidine biosynthesis pathway whose structure remains to be determined (V. J. Davisson, personal communication). The HisI PR-AMP-cyclohydrolase exists as a dimer that requires both Zn^{+2} and Mg^{+2} ions for catalysis (69, 200), although Cd^{+2} can replace Zn^{+2} with some change in catalytic properties. The active site of the PR-AMP-cyclohydrolase is formed by the dimer interface, and each Zn^{+2} is bound by three conserved Cys residues, one from one subunit and the other two from the other subunit (200) The Zn^{+2} ions bind with high affinity and likely play a direct role in catalysis by activating a water molecule, similar to the mechanism in nucleoside/nucleotide hydrolases (200). The Mg^{+2} ion is freely exchangeable, and there may be co-binding of Mg^{+2} and the substrate (69) Mg^{+2} is bound by conserved aspartate residues in the cleft of the active site, and Mg^{+2} may also play a role in the catalytic mechanism (200).

HisA—The fourth step of histidine biosynthesis is carried out by the HisA enzyme (Fig. 1). HisA catalyzes an Amadori rearrangement that leads to the irreversible isomerization of the aminoaldose Pro-FAR substrate to a more stable aminoketose product (see above and Fig. 1) (113). The structure of HisA is a $(\beta\alpha)_8$ barrel structure, which is a common fold shared by many enzymes, including other sugar isomerases, such as the TrpF enzyme involved in tryptophan biosynthesis (see (113, 129, 142, 145)). HisA and TrpF share almost no amino acid similarity, but remarkably, a single amino acid change in HisA (Asp127Val) imparts TrpF enzymatic activity (129). Like other $(\beta\alpha)_8$ barrel enzymes, the active site of HisA is located on the C-terminal ends of β strands, which form an inner parallel β-sheet. In HisA, aspartate residues at the C-terminal ends of β-sheets 1 and 5 are required for catalytic activity (113, 145). The Asp127Val mutation in HisA is thought to change the catalytic specificity by allowing the more negatively charged TrpF substrate to bind to the HisA active site (145). Kinetic and mutagenesis analyses have been performed on the HisA and TrpF enzymes of *Thermotoga maritima* and *E. coli* (113). These combined biochemical and structural studies suggest that the HisA and TrpF isomerases share a common catalytic mechanism that involves general acid-base catalysis (113). In addition, both enzymes seem to have high catalytic turnover that allows rapid consumption of their relatively unstable aminoaldose substrates. Finally, the extraordinary plasticity of $(\beta\alpha)_8$ barrel enzymes was reiterated by the demonstration that a single mutation (Asp130Val) caused the *T. maritima* IGP synthase HisF subunit, which is folded into a $(\beta\alpha)_8$ barrel structure, to acquire TrpF isomerase activity (145). These finding supports the notion that the reaction specificities of current $(\beta\alpha)_8$ barrel enzymes evolved from an ancestral enzyme of broad substrate

specificity (129, 145). An important corollary of this idea is that $(\beta\alpha)_8$ barrel enzymes might be engineered to acquire new activities (129).

HisH-HisF heterodimer—The HisH-HisF IGP synthase catalyzes the fifth step of histidine biosynthesis (Fig. 1; (10, 11, 136, 137, 164, 165)). HisH-HisF is a class I glutamine amidotransferase, which carries out two concerted reactions. The HisH subunit contains a flavodoxin-like fold and is a glutaminase that produces a protected ammonia molecule from glutamate (see (164)). The HisF subunit, which is folded into an $(\alpha\beta)_8$-barrel structure, uses this ammonia in a carbon-nitrogen ligation and cyclization reaction that produces IGP and AICAR (Fig. 1) (164). The HisH-HisF IGP synthase was the last step worked out in the histidine biosynthesis pathway (137) and is noteworthy, because it carries out its reactions by a concerted allosteric mechanism that channels the ammonia product formed by the HisH subunit to the PRFAR substrate in the active site of the HisF subunit (see (11, 164)). No additional intermediates are synthesized by HisH in the absence of HisF, as was initially proposed (see (137)).

The concerted allosteric regulation and metabolic channeling prevent waste of glutamine and protect the ammonia molecule for the second step in the reaction (see (11, 164)). The current model for the mechanisms of catalysis, regulation, and channeling are based on the structures of the enzyme from yeast (61, 165) and *Thermotoga maritima* (80), biochemical analyses, and extensive modeling approaches (see (11, 164)). Briefly, glutamine is thought to bind to the HisH active site that contains a conserved cyteine-histidine-glutamate triad that catalyzes glutamine hydrolysis (164). Yet, the HisH glutaminase remains essentially inactive until the other substrate, PRFAR, binds to the active site of the HisF barrel, which is about 30 Å away. PRFAR binding to HisF stimulates the rate of the distant HisH glutaminase by about 5,000-fold to a robust $k_{cat} \approx 7\ s^{-1}$ (11, 165). PRFAR binding occurs by electrostatic interactions to the C-terminal face over the hole of the HisF beta barrel. Binding of PRFAR induces an ordering of an unstructured loop in HisF that is communicated directly to the interface between the HisH and HisF subunits by a network of evolutionarily conserved residues. Subsequent formation of a key salt bridge leads to tightening of the interface between the subunits into a closed conformation, which opens an internal channel and increases the rigidity of the HisH active site, thereby stimulating cleavage of glutamine. Released ammonia is relayed from the HisH active site across the interface to the core of the HisF-beta barrel by the network of conserved residues, which exclude water. Following the cyclo-ligase reaction catalyzed by HisF, release of the IGP and AICAR products is thought to disrupt salt-bridges and hydrogen bonds in the subunit interface and loosen the subunit interface. Glutamate can then exchange from the HisH active site for a new glutamine substrate molecule, and the enzyme is set for another round of concerted reactions.

Recently, it was reported that acivicin, which is a natural product analog of glutamine, prevents the growth of *E. coli* in minimal medium (202). Acivicin is produced by *Streptomyces sviceus* and is being tested as an antitumor compound based on its inhibition of mammalian amidotransferases (see (116)). Growth of *E. coli* was restored by the addition of purines or histidine, which suggested that acivicin was inhibiting the HisH-HisF IGP synthase. Enzyme assays containing purified HisH-HisF confirmed that acivin is a potent

inhibitor of IGP synthase (202). Other studies showed that acivicin inhibits HisH-HisF activity by a mechanism-based formation of a covalent bond between acivicin and the active-site Cys residue of HisH (64). Interestingly, inactivation is enhanced by binding of the PRFAR substrate to HisF, presumably by the same allosteric mechanism that activates the glutamine cleavage (64). Microarray analyses of transcripts levels in bacteria treated with the drug confirmed a block in histidine biosynthesis, including induction of stringent response, but also showed a complex pattern of transcript changes, indicative of other targets (202).

There is one other long-standing, curious observation concerning the HisH-HisF IGP synthase. Overexpression of HisH-HisF is highly pleiotropic and inhibits cell division of *E. coli* and *S. typhimurium*, particularly in the presence of high concentrations of sugar sources (102, 163). Induction of the SOS response or production of AICAR cannot account for these defects (93, 102). It was suggested that HisH-HisF overproduction may cause a partial block in cell septum formation (98). This idea was supported by the observation that D-cycloserine suppresses the filamentation caused by HisH-HisF overexpression (47). D-cycloserine inhibits D-alanine ligase and racemase, thereby curtailing production of complete five amino acid stem peptides. Therefore, peptidoglycan precursor amount is somehow linked to the filamentation of HisH-HisF mutants, but the mechanism remains unclear. Finally, it had been noted that some strains of *S. typhimurium* form filaments inside of host cells, such as macrophages (115). Strains which have these growth defects contain a non-polar mutation in *hisG* and the growth-arrest phenotype depends on HisH-HisF expression (115). Likewise, some mutations outside of the *his* operon that lead to filamentation inside of host cells, such as Δ*trpC* insertions, also depend on possible HisH-HisF over-expression. However, it is not clear whether triggering the *his* operon to overexpress HisH-HisF and inhibit bacterial cell division plays any role in host defense.

Bifunctional HisB—The C-terminal and N-terminal domains of HisB protein catalyze the sixth (IGP dehydratase) and eighth (Hol-P phosphatase) steps, respectively, in the histidine pathway (Fig. 1 and above). The two domains seem to function independently and are found as separate enzymes in many other species (see (181)). Fusion to form bifunctional HisB has been proposed to be a recent evolutionary event (45). The structure of the monofunctional IGP dehydratase was determined from the fungus *Filobasidiella neoformans* (197), and the structure of the N-terminal domain of HisB (HisB-N) was determined for *E. coli* (181).

The IGP dehydratase removes a non-acidic hydrogen atom from IGP (Fig. 1), which contrasts to the leaving hydrogen in most other dehydratase reactions (197). IGP dehydratase does not show any amino acid similarity with other known proteins and has the unusual property that it requires Mn^{+2} ion for activity and formation of higher 24-mer oligomeric structures (197). In the absence of Mn^{+2}, IGP dehydratase crystallizes as a trimer in which each monomer contains a compact domain that is formed by half-domains of an unusual topology (197). Each half-domain contains a histidine-rich motif that is highly conserved in IGP dehydratases. The two half domains likely arose by a duplication event. Modeling of the trimer into a 24-mer places the conserved sites into one site that likely is the Mn^{+2} binding site and possibly the active site (197). The structure of IGP dehydratase has allowed a better understanding of the aggregation state of bifunctional HisB in *E. coli* and *S.*

typhimurium (see below). In addition, plant IGP dehydratase is a target for herbicides, and the structure will further efforts to improve the potency and specificity of these chemicals (103, 191).

In contrast to monofunctional IGP dehydratase, the HisB-N domain, which catalyzes HolP phosphatase in the presence of divalent cations, forms a dimer in solution and crystals (181). However, the intact bifunctional HisB protein forms large aggregates in the presence of Mn^{+2} due to oligomerization of the HisB-C IGP dehydratase domain (181, 197). Importantly, oligomerization of the intact HisB protein does not affect the Hol-P phosphatase activity. A model based on the structures of the individual HisB-N and HisB-C domains was constructed (181). In this model, bifunctional HisB forms a 24-mer in which the HisB-N and HisB-C domains are matched, and hexamers are the basic unit within the structure.

The structure of the dimeric His-N phosphatase domain was determined in the presence of Mg^{+2} ion, Ca^{+2} ion, Mg^{+} + histidinol, Ca^{+2} + pAsp, or Mg^{+2} + sulfate ion. These different structures represent “snapshots” of various intermediates in the phosphatase reaction pathway. Each monomer of HisB-N folds into a single domain with the structure of a haloacid dehalogenase (HAD) superfamily enzyme (45, 181). Each monomer contains the four invariant aspartate residues (DDDD) involved in catalysis, which proceeds through a phosphoaspartate intermediate. Zn^{+2} ion stabilizes an extended loop in the HisB-N structure. The active site contains two divalent cation binding sites, and the phosphatase is active in the presence of Mg^{+2}, Mn^{+2}, Co^{+2}, or Zn^{+2}, but is inhibited completely by Ca^{+2}. The structures suggest that the second bound divalent cation participates in the reaction mechanism, which is different from other characterized HAD enzymes (181). The proposed mechanism also suggests how Ca^{+2}ion, which has a relatively large atomic radius, binds to the two metal binding sites, distorts the active site, and arrests the reaction after formation of the phosphoaspartate intermediate.

HisC—Aminotransferases homologous to HisC are widespread in amino acid biosynthetic pathways and catalyze the transfer from glutamate of an amino group that eventually becomes the α-amino group in the amino acid end product of the pathway (Fig. 1 and above). Aminotransferases use the vitamin B_6-derived coenzyme pyridoxal 5’-phosphate in a reaction mechanism involving formation of a Schiff’s base (see (111, 158, 199) and Chapter XX). The structure of the *E. coli* HisC aminotransferase, which catalyzes the seventh step of histidine biosynthesis (Fig. 1), was determined complexed with pyridoxamine 5’-phosphate, as an internal covalent aldimine with pyridoxal 5’-phosphate, or as a covalent complex with pyridoxal 5’-phosphate and HolP (199) or complexed with HolP or *N*-(5’-phosphopyridoxyl)-L-glutamate (111). HisC exists as a dimer, and each monomer consists of a larger α/ β/ α domain that binds pyridoxal 5’-phosphate, a smaller domain, and an N-terminal dimerization arm (111, 199). The residue forming the Schiff’s base with PLP is Lys214 or Lys217 in *E. coli* or *S. typhimurium* HisC, respectively, and the HolP substrate binds in the dimer interface at a site that partially overlaps the glutamate binding site (199). The spectroscopic properties of wild-type and mutant HisC are consistent with the idea that bond strain within the Shiff’s base lowers its pK_a and contributes to catalysis (158).

The structure of HisC is similar to that of other aminotransferases, despite weak homology at the amino acid level, and amino acids involved in pyridoxal 5'-phosphate binding, substrate binding, catalysis, and dimerization are conserved in different aminotransferases (111, 199). Binding of Hol-P, pyridoxamine 5'-phosphate, or pyridoxal 5'-phosphate to HisC does not cause large structural changes in the protein or ligands (199). The covalent tetrahedral complex formed between HisC, pyridoxal 5'-phosphate, and HolP resembles a gem-diamine structure, which is an expected intermediate in the reaction (199). This is the first report for any aminotransferase of the structure of this normally transient intermediate, which may have been stabilized by crystal packing forces (199). Finally, amino acid sequence and protein structure comparisons suggest that the HisC aminotransferase is closely related to the PLP-dependent CobD decarboxylase from the cobalamin biosynthetic pathway of *S. typhimurium*, suggesting a common evolutionary origin (62, 63). In addition, the HisC HolP aminotransferase from *Thermotoga maritima* has evolved the ability to bind aromatic amino acids and functions both as a HolP and aromatic amino acid aminotransferase (88).

Bifunctional HisD—HisD catalyzes the final two steps of histidine biosynthesis (Fig. 1 and above). The crystal structure of the HisD homodimer unbound and bound to the substrate histidinol and cofactors NAD^+ and Zn^+ has been recently reported (26). This paper also reviews the proposed reaction mechanism of the four-electron oxidation reaction catalyzed by HisD (26, 210). Each monomer of the HisD dimer consists of four domains; two make up a globule structure containing incomplete Rossmann folds, and two make up a tail-like structure. The dimer is formed by domain swapping in the tail structures. The incomplete Rossmann folds, some sequence similarity, and tandem arrangement suggest that the two domains in the globule structure arose by a duplication event. The active site of the enzyme is formed by amino acids from both of the monomers that form the dimer. One of the Rossmann folds is involved in NAD^+, binding, whereas the other Rossmann fold binds Zn^{+2} ion and the substrate histidinol. Zn^+ functions in substrate binding, but not catalysis, and is required for histidinol substrate binding. NAD^+ binds relatively weakly to the Rossmann fold in an unusual way compared to a canonical NAD^+-Rossmann fold structure (26). The structures of HisD are consistent with a mechanism for HisD catalysis that was proposed earlier based on kinetic and biochemical studies of wild-type and mutant HisD proteins (210). This acid-base catalysis mechanism involves four bases, including conserved histidine residues (26, 210). The crystal structure also refines the stereochemistry of the NAD^+ reactions.

STRUCTURE AND REGULATION OF THE his OPERON

The *his* operon located at 42 min in the *S. typhimurium* chromosome is depicted in Fig. 2. The *S. typhimurium* and *E. coli his* DNA sequences are 81% identical, and the structure of the *E. coli his* operon at 44 min (2) is essentially the same as that of *S. typhimurium*, with the exception of a repetitive extragenic palindromic (REP) sequence between *S. typhimurium hisG* and *hisD* and several other minor differences (49). The locations of some *his* regulatory loci genes are also listed in Table 1. Parameters relevant to *his* operon structure and control are collected in Table 3 and have not changed since the last version of this review. They give the following general picture of the operon. The eight structural genes are transcribed

into a single, polycistronic mRNA molecule (Table 3) (49, 153), which extends from the primary promoter (*hisp1*) to the strong, bidirectional Rho-independent terminator (Fig. 2). The frequency of transcription initiations at *hisp1* is positively regulated by a limited range of intracellular ppGpp concentrations. New results indicated that this stimulation by ppGpp occurs by a direct mechanism (66, 175). An RNA polymerase molecule that initiates transcription at *hisp1* first transcribes a leader region and must continue transcribing past the attenuator control site if it is to enter the first structural gene (*hisG*) of the operon. The *hisp1* promoter, leader region, and attenuator are contained in a genetic locus which traditionally has been designated the *hisO* region, even though the operon is not controlled by a classical repression mechanism (Fig. 2 and 3). Transcription termination or readthrough at the *his* attenuator will occur when the percentage of $tRNA^{His}$ charged with histidine is high (88%) or low (≈12%), respectively (126, 132, 146). In addition, the percentage of transcription termination may be modulated indirectly by chromosome DNA supercoiling density, which is set by the total cellular concentration of $tRNA^{His}$ molecules (90, 169, 187). Transcription termination at the *his* attenuator produces a terminated leader transcript of approximately 180 nucleotides (nt), which extends from *hisp1* to a site in the attenuator region (59, 99). In some instances, transcription initiation can occur at two internal promoters (*hisp2* and *hisp3*, Fig. 2) located before the start of the *hisB* and *hisI* genes; however, transcription from *hisp1* occludes expression from *hisp2 in vivo* (5). The polycistronic *hisOGDCBHAFI* primary transcript is processed in several discrete endonucleolytic steps (Fig. 2 and Table 3) (5). The processed transcript containing *hisBHAFI* has a chemical half-life of about 15 min and is much more stable than the *hisOGDCBHAFI* primary transcript, whose half-life is about 4 min (5). These features of *his* operon structure and regulation are described in detail in the next sections.

Structure of the his Operon

The Primary Promoter hisp1—Figure 3 presents the nucleotide sequence of the S. typhimurium *hisO* region (25, 29, 49, 184). The start of transcription determined *in vitro* and *in vivo* and the corresponding -35 and -10 regions for binding of σ^{70} RNA polymerase are indicated (29, 49, 78, 99, 100). There is an AT-rich “discriminator” sequence between the -10 box and the +1 start of transcription that is required for ppGpp stimulation of transcription from *hisp1* (70, 184). The nucleotide sequence of the *E. coli hisp1* promoter is identical to that of the *S. typhimurium* promoter in its -35 and -10 regions and is similar in the 18-nt -30 to -14 spacer and in the -6 to +1 discriminator region. The start of transcription at the *E. coli hisp1* promoter *in vivo* and *in vitro* is analogous to the position indicated in Figure 3. *his-lac* fusions were used to identify mutations that decrease the efficiency of the *hisp1* promoter by 4- to 400-fold compared with the wild-type promoter. These down mutations alter the sequences of the -35 or -10 regions or the spacing between these two regions and thereby confirm the position of *hisp1* (25). The *hisp1* promoter is unusually strong *in vivo* and *in vitro* on supercoiled templates (218). The *E. coli hisp1* promoter was cloned into a *galK* expression vector and found to be about four times stronger than the *gal* promoter *in vivo* (180). The strength of *hisp1 in vivo* is further indicated by the result that the histidine biosynthetic enzymes amount to at least 4% of the total cellular proteins in bacteria deleted for the *his* attenuator (174). Results from *in vitro* experiments confirm that *hisp1* is stronger than a pBR322 promoter and show that transcription from *hisp1* is about

20-fold stronger on supercoiled templates than on linear templates (218). However, *his-lac* expression from a mutant lacking the *his* attenuator is decreased slightly by high osmolarity and anaerobiosis, which are thought to increase chromosomal negative supercoiling (169). The inference from this result is that transcription from *hisp1* is not strongly affected by the changes in chromosomal DNA supercoiling density that occurs *in vivo* in response to physiological conditions. The effects of ppGpp on transcription from the *hisp1* promoter are discussed below.

The Internal Promoters hisp2 and hisp3—The positions of two internal promoters have been evolutionarily conserved in the *his* operons of *E. coli* and *S. typhimurium* (49, 106, 189). By using Tn*10* insertions to block transcription from upstream regions in the *S. typhimurium his* operon, *hisp2* was initially mapped near the end of the *hisC* coding region before the start of *hisB* and *hisp3* mapped near the end of the *hisF* coding region before the start of *hisI* (189). The *S. typhimurium* and *E. coli hisp2* promoters were S1 mapped at about 100 bp upstream from the end of the *hisC* coding region (106), very close to a major processing site of the *his* primary transcript (5). Experiments in which transcription from *hisp2* was measured in mutants lacking transcription from *hisp1* or in which transcription from *hisp1* or *hisp2* was measured in *galK* expression vectors showed that *hisp2* is about half as strong as *hisp1* (84, 106). This relatively strong expression contrasts with the low (<10%) expression from *hisp2* observed *in vivo* compared with the amount of *his* primary transcript initiated at *hisp1* and transcribed through the attenuator (5). An indirect method based on ratios of enzyme activities suggested that transcription from *hisp2* is insignificant when transcription of the *his* structural genes is equal to or greater than the level found in wild-type bacteria (84). Together, these results imply that transcription of *hisp2* is occluded by transcription from *hisp1*. This hypothesis has been confirmed by studies showing that the level of *hisp2* transcription is inversely correlated with the amount of readthrough transcription beyond the *his* attenuator (5).

The internal promoter in the *trp* operon is thought to maintain sufficient levels of the TrpC and TrpB polypeptides, each of which contains multiple tryptophan residues. The TrpE and TrpD polypeptides, which are encoded by genes upstream from the internal promoter, contain few tryptophan residues and would not be seriously depleted by sudden tryptophan starvation (225). An analogous function for the *hisp2* and *hisp3* internal promoters seems unlikely because the HisG polypeptide, which is encoded by the first gene in the operon, contains multiple histidine residues (49, 177). In both *E. coli* and *S. typhimurium*, the *hisp2* promoter is metabolically regulated (106, 222); however, the physiological functions of the *his* internal promoters remain unknown. This mystery is compounded by the fact that the promoter-distal segment of the primary *his* transcript is processed into a long-lived *hisBHAFI* transcript that contains the same intact genes as transcripts initiated at the *hisp2* promoter (5). It would seem that for some unknown physiological reason, *E. coli* and *S. typhimurium* evolved mechanisms to maintain expression of the last five genes of the *his* operon (5).

his operon structural genes and evolution—The complete DNA sequences of the *E. coli* and *S. typhimurium his* operons have been determined and compared (25, 29, 46, 48, 49,

105, 183). The *his* operons of both species are extremely compact, except for the expected space between the end of the *his* leader peptide and *hisG* and in the *hisG-hisD* intercistronic region. In fact, there is only one small 5-bp intercistronic region between *hisG* and *hisD* in the entire 7,379-nt *E. coli his* operon; for all the other gene pairs, the translation stop codon of the upstream gene overlaps the translation initiation codon of the next downstream gene (49). Likewise, except for *hisG* and *hisD*, the reading frames of all of the *S. typhimurium his* genes overlap. The ≈100-nt *S. typhimurium hisG-hisD* border contains a REP DNA sequence that is found throughout the bacterial chromosome (49, 117, 207). The absence of a REP sequence in the *E. coli hisG-hisD* intercistronic region supports the idea that such sequences arose through transposition (117). The *S. typhimurium hisG-hisD* REP sequence has been shown to act as a joining point for chromosomal rearrangements, including the generation of tandem duplications in *recA*$^+$ bacteria (195).

Overlapping of translational signals raises the possibility that extensive translational coupling occurs during the expression of the *his* operon. In the *trp* operon, translational coupling between the *trpE* and *trpD* genes is thought to guarantee equimolar synthesis of the corresponding gene products, which interact to form a multimeric enzyme (225). In *S. typhimurium*, the HisG, HisD, HisC, and HisA polypeptides are expressed in molar ratios of 3:1:1:1 (221). Because of the large intercistronic region, direct translational coupling would not be expected between *hisG* and *hisD*. Some level of translational coupling between other genes in the operon could produce the equimolar synthesis of the HisD, HisC, and HisA polypeptides detected *in vivo*. Translational coupling might also influence the kinetics of *his* operon expression after the onset of histidine limitation; perhaps the sequential appearance of the histidine biosynthetic enzymes in cells with low formylating capacity reflects translational coupling, whereas the simultaneous appearance of the histidine biosynthetic enzymes in cells with high formylating capacity indicates a mode of uncoupled, independent translation (32). Unfortunately, whether translational coupling occurs in the *his* operon expression remains unresolved (49).

Numerous recent studies have analyzed the distribution and evolution of the *his* operon and histidine biosynthetic genes. A couple of generalizations can be drawn from these reports that are relevant to this review. Compact attenuation-regulated *his* operons similar to those of *E. coli* and *S. typhimurium* occur in γ-proteobacteria, including pathogenic *Yersinia* and *Vibrio* species (219); however, there are orders of γ-proteobacteria, such as *Pseudomonas* species, whose histidine biosynthetic genes are scattered around the chromosome and that lack obvious attenuation control (219). This variety of structures and regulation is also evident in gram-positive bacteria, which contain different patterns of *his* gene arrangements and regulation, including histidine-specific T-boxes (219). Moreover, some species within an order synthesize histidine (e.g., *Streptococcus mutans*), whereas other species do not contain histidine biosynthetic genes (e.g., *Streptococcus pneumoniae*).

Two scenarios have emerged for the evolution of unified, compact *his* operons, such as those of *E. coli* and *S. typhimurium*. One analysis was based only on *his* gene arrangements in proteobacterial species (86). According to this scenario, ancestral *his* genes encoded monofunctional enzymes and were scattered throughout the chromosome. These separate *his* genes then underwent a series of joining steps that built highly compact *his* operons, such as

those present in *E. coli* and *S. typhimurium.* These compact *his* operons then transferred horizontally among proteobacterial species (86). A later study included the organization of *his* genes from phyla outside of the Proteobacteria (179). The major conclusion from this analysis was that the compact *his* operon is widely distributed and ancient (179). According to this scenario, the unified *his* operon emerged early, was transferred horizontally, and was subsequently broken up in some bacterial species. Beyond this difference in conclusions about the origin of the unified operon, other analyses persuasively argue that gene elongation events (HisA), gene duplications (HisA and HisF), and gene fusions (leading to biofunctional HisI and HisB proteins) occurred during the evolution and assembly of the histidine biosynthetic pathway in *E. coli* and *S. typhimurium* (see (85)).

his operon expression and intracellular formylating capacity—A limited number of studies suggest that intracellular formylating capacity and its modulation of initiator fMet-tRNA pools may influence *his* operon expression (see (7)). Premature transcript 3′ ends were mapped in the *hisC* region in response to the drugs trimethoprim and kasugamycin, which decrease the intracellular fMet-tRNA pool and the binding of fMet-tRNA to ribosomes, respectively, and thereby uncouple transcription and translation (7). Both antibiotics lead to premature *his* transcript release, possibly by increasing Rho factor-dependent transcription termination within the operon (see below) and RNA polymerase pausing (7). Trimethoprim, and to a lesser extent kasugamycin, also led to an increase in *his* transcript processing in the *hisC-hisB* region (7), possibly by exposing a transcript processing site within *hisC* or by fostering ribosome stalling at the start of *hisB* (see below). Another link between histidine biosynthesis and intracellular formylation involves production of AICAR (Fig. 1), which must be formylated to reenter the nucleotide pool (7, 36). Increased AICAR production may reduce intracellular formylating capacity (7, 32), and this reduction may account for the increased *his* transcript release and processing observed in *his* constitutive and nonpolar *hisD* and *hisC* mutants (7).

his transcript processing by RNaseE and RNaseP—Three major processed *his* transcripts were detected by Northern (RNA) blotting (Fig. 2 and Table 3). Processing of longer transcripts to form the 3,900-nt *hisBHAFI* transcript was studied in detail and shows some remarkable features (5, 8). The processed *hisBHAFI* transcript is extraordinarily stable ($t_{1/2} \approx$ 15 min) compared with the full-length *his* operon transcript ($t_{1/2} \approx$ 4 min) (Table 2) (5). A cis element in *hisC* upstream from the processing point is required for efficient transcript cleavage (5, 8). This cis element was recognized specifically by an RNA-binding protein in gel shift assays (5) and probably binds RNaseE or an endoribonuclease associated with RNaseE (8). In addition, RNaseE probably cuts the full-length transcript at several other sites within the *hisC* region (8). Ribosome binding to the translation start site of *hisB*, which is the first complete gene in the processed transcript, also was required for efficient processing and transcript stability (5, 8). Recent data support the model that the initial RNaseE cut in *hisC* and ribosome binding at the start of *hisB* cause the processed transcript to assume a specific secondary structure that is further cut by RNaseP (8). This is the first report implicating the RNaseP ribozyme, which mainly cuts pre-tRNA, in mRNA processing. The resulting *hisBHAFI* transcript has a 5′-end hairpin structure, which together with translation of *hisB* may enhance the stability of the 3,990-nt mRNA fragment. The

processing pattern of the *his* primary transcript needs to be reconciled with the 3:1:1:1 stoichiometry of the HisG, HisD, HisC, and HisA polypeptides. The greater stability of the *hisBHAFI* processed transcript than of transcripts that contain other *his* genes, such as *hisD*, raises the issue of how equimolar amounts of HisD, HisC, and HisA polypepties are maintained, if the *hisBHAFI* transcript is indeed translated. Finally, the processing site between *hisG* and *hisD* (Fig. 2) and the presence of a REP sequence that can stabilize mRNA from 3′→ 5′ endonucleolytic attack (123) suggest one mechanism that could account for the higher amount of HisG protein than other *his* proteins in *S. typhimurium* (221).

A recent report suggests another role for RNaseP endonuclease processing of the *his* primary transcript (147). At a nonpermissive temperature, a temperature-sensitive mutant of RNaseP accumulated *his* mRNA extending from a region in front of *hisG* to the end of the operon (Fig. 1). However, transcripts corresponding to the *hisO* leader region did not accumulate in the mutant, and an RNaseP cleavage site was mapped to the intercistronic region between the *hisO* leader region and the start of *hisG* (147). This study also confirmed the RNaseP cleavage site near *hisC* mentioned above (8). Analogous RNaseP cleavage sites were detected in other operons (147) suggesting that RNaseP cleavage may control the stability of transcripts downstream from cut sites. Further studies of this phenomenon are needed for the *his* operon, especially direct demonstration that the accumulation is independent of $tRNA^{His}$ amount and attenuation control.

Rho factor-dependent “classical” polarity within the his operon and roles of NusA and NusB—Mapping of cryptic transcription termination points within the *his* operon has provided an explanation for the strong gradient of classical polarity observed for *hisG*, but not for other *his* genes, such as *hisD* and *hisA* (3, 6). Nonsense mutations early, but not later in *hisG*, strongly reduce expression of downstream genes in the *his* operon; by contrast, nonsense mutations located throughout *hisD* and *hisA* strongly reduce downstream *his* operon expression (3, 6, 91). Premature translation termination within a coding region exposes potential mRNA targets to entry of Rho factor, which causes the premature transcription termination that underlies the decrease in downstream gene expression (3, 6). These Rho factor-dependent sites have been designated as transcription termination elements (TTEs) for the *his* operon (50). According to this model, the TTEs lie downstream of the premature translation stop codon and contain a transcription pause site which becomes the 3′ transcript end produced by Rho-dependent transcription termination. Each TTE in the *his* operon also contains a cytosine-rich and guanosine-poor region upstream from the pause site that serves as an entry for binding of the Rho factor hexamer. The locations of these TTEs correspond to the polarity patterns observed for *his* operon nonsense mutations. The only TTEs in *hisG* are located early in the gene; therefore, only nonsense mutations upstream of these entry sites are strongly polar. In contrast, TTEs are located throughout *hisD* and only at the end of *hisA*; therefore, nonsense mutations essentially anywhere within *hisD* or *hisA* are upstream of a TTE (6). The polarity pattern within *hisC* is complicated by the transcript processing mentioned above. It is not clear whether the putative translational coupling described above might also contribute to the strong polarity gradient observed in *hisG* in contrast to the uniform polarity observed in the internal genes of the *his* operon (3, 6, 91).

Further study of transcription termination at TTE1 and TTE2 from *hisG* in the absence of translation revealed that the NusA and NusB transcription elongation factors modulate polarity at these sites. TTE2 is the stronger Rho-dependent termination site and functions independently of the NusB factor *in vitro* (50). In contrast, the suboptimal TTE1 site is preceded by a BoxA sequence, which binds to NusB and enhances transcription termination at TTE1 by Rho factor *in vivo* and *in vitro* (50). This finding was unexpected, because the NusB factor often acts as an antitermination factor. Further studies suggested an involvement of NusA and NusE along with NusB on efficient termination at TTE1 (51). This study also showed that NusA increases the efficiency of termination at TTE2 by increasing transcription pausing. A last interesting result from this study is that NusA is required even when there is normal translation of the *his* operon. Mutants deficient in NusA function showed increased transcription termination at the TTE2 site suggesting that NusA modulation of transcription elongation may be important in maintaining tight coupling between transcription and translation (51). Finally, the *his* TTE1 and TTE2 sites have been used in screens of potential antibiotics that inhibit Rho factor (53, 54).

The terminator at the end of the his operon—Transcription termination at the end of the *E. coli* and *S. typhimurium his* operons occurs at strong Rho factor-independent terminators (48, 52). The *S. typhimurium* terminator is located only a few nucleotides downstream from the *hisI* stop codon, whereas the *E. coli* terminator is preceded by a nontranslated region of 40 nt (49). The *S. typhimurium his* terminator is a symmetrical, mirror-image structure; each strand contains (reading 5′ to 3′) a G+C-rich inverted repeat followed by several T residues. This mirror-image structure suggested that the terminator might function in both orientations. This prediction was confirmed both *in vivo* and *in vitro* (52). Analysis of *in vivo* transcription termination points by S1 mapping and Northern hybridizations demonstrated that this structure terminates *his* operon mRNA initiated at the *his* primary and internal promoters and, at the same time, terminates a 1,200-nt-long transcript synthesized from the DNA strand opposite to the one copied into *his* mRNA. The gene convergent to the *his* operon was identified as *rol*, which regulates the size distribution of the O-antigen moiety of lipopolysaccaride (Fig. 2) (31). Both the *his* and *wzz* (*rol*) transcripts synthesized *in vivo* end with polyuridylate residues, as expected for Rho factor-independent transcription termination. The *his/wzz* terminator functions at greater than 90% efficiency in either orientation *in vivo*, and it does not seem likely that there is any regulatory connection between the *his* operon and *wzz* gene through this shared terminator. The Rho factor-independent nature and high efficiency of the *his/wzz* terminator in both orientations were confirmed in a purified *in vitro* transcription system.

Regulation of his Operon

Metabolic regulation—As noted above, *his* operon expression is about four fold greater in bacteria growing in minimal-glucose medium than bacteria growing in rich medium (Table 2). This inverse relationship between *his* operon expression and cellular growth rate is a form of metabolic regulation that adjusts *his* operon expression in response to the general amino acid supply in the cell (176, 205, 222). Because ppGpp levels were known to vary inversely with growth rate (see Chapter XX), ppGpp was examined as a possible positive effector of *his* operon expression. In an *in vitro* coupled transcription-translation

system prepared from a *relA*$^-$ mutant defective in ppGpp synthesis (see Chapter XX), addition of 100 μM ppGpp caused a 10-fold increase in expression of the wild-type *his* operon contained on a linear, transducing phage template (205). Equal levels of ppGpp-mediated stimulation were detected from the wild-type template and from a mutant template deleted for the *his* attenuator, which showed that ppGpp acts independently of attenuation. By uncoupling transcription and translation in the *in vitro* system, it was possible to show that ppGpp stimulates *his* operon transcription but not translation. From these results, ppGpp was postulated to be the effector molecule that directly mediates metabolic regulation of *his* operon expression (205).

Results from physiological experiments strongly support the model for the role of ppGpp as a positive effector of *his* operon expression. The increase in expression of the *his* operon in bacteria subjected to sudden histidine starvation in amino acid-rich medium is markedly less in *relA*$^-$ mutants than that in *relA*$^+$ strains (205). There is a positive correlation between *in vivo his* operon expression and intracellular ppGpp concentrations, up to the ppGpp level found in bacteria growing in minimal-glucose medium (186, 205, 222, 223); increases in *in vivo* ppGpp concentrations beyond this level fail to increase *his* operon expression (222). These results support the notion that *his* operon transcription is maximally stimulated at lower than maximum *in vivo* ppGpp concentrations. Positive control of *his* operon expression by ppGpp was strongly confirmed by genetic schemes in which mutants defective in ppGpp metabolism were selected on the basis of growth characteristics in the presence of histidine analogs that inhibit histidine biosynthesis (see below) (186). Experiments were performed in which intracellular ppGpp was drastically reduced below the level found in *relA*$^+$ bacteria growing in rich medium (193). Results from this study show that attenuator-independent *his* operon expression decreases about 15-fold in a *relA*$^-$ mutant and increases about 2-fold in a *relA*$^+$ strain in response to the decreased and increased ppGpp levels, respectively, induced by addition of the analog serine hydroxamate to the amino acid-rich growth medium. Thus, the full range of the ppGpp-mediated metabolic regulation of *in vivo his* operon expression is at least 30-fold. Finally, a number of physiological experiments have confirmed the conclusion that ppGpp-mediated metabolic regulation and attenuation are independent mechanisms for the control of *his* operon transcription (182, 184, 186, 193, 222, 223). A corollary of this conclusion, that starvation for amino acids other than histidine increases transcription of the *his* operon, has been confirmed (222). In these experiments, the amino acid limitation should not have interfered directly with leader peptide synthesis in a way that would increase read-through transcription of the *his* attenuator (see below). ppGpp-mediated metabolic regulation induces the expression of several other amino acid biosynthetic operons besides the *his* operon (55, 205). These earlier results were recently confirmed by microarray analyses of the *E. coli* stringent response, which activated the transcription of leader transcripts of several amino acid biosynthetic operons, including *hisL* (81). In this regard, it is particularly noteworthy that *relA spoT* double null mutants show a complex requirement for amino acids that can be met by high concentrations of Casamino Acids (224). The effect of ppGpp accumulation on HisG enzyme activity, which controls the flow of intermediates through the histidine biosynthetic pathway, was described above.

One of the most interesting questions about *his* operon metabolic regulation concerns the mechanism by which ppGpp stimulates transcription. In early studies, strains containing putative mutations in the *hisp1* promoter showed altered levels of attenuator-independent *his* operon expression in response to amino acid downshifts (222). These results suggested that ppGpp affects transcription initiation frequencies at the *hisp1* promoter; but, more rigorous interpretations were not possible at that time because the base changes of the mutations were unknown. Two lines of investigation have served as prelude to recent definitive experiments on the mechanism of ppGpp stimulation of *his* operon transcription. Systematic studies by Artz and coworkers of *his* promoter mutations *in vitro* in a coupled transcription-translation system and *in vivo* in the bacterial chromosome showed similar results and strongly suggested that stimulation of *his* operon expression by ppGpp occurs at or near the *hisp1* promoter (70, 184). In addition, stimulation of ppGpp of *hisP1* transcription depends on the sequence of the -10 region in the promoter and an AT-rich discriminator region between the -10 box and the start of transcription. For example, site-directed mutations that increase the matches of the -10 region of the *hisp1* promoter to the consensus for a σ^{70}RNA polymerase promoter increased transcription from *hisp1* in the absence of ppGpp and largely abolished the stimulation measured from the wild-type promoter in response to ppGpp both *in vitro* and *in vivo* (70, 184).

Paradoxically, earlier attempts to detect activation of transcription by ppGpp in purified *in vitro* transcription systems proved to be largely unsuccessful (27, 28). Therefore, it was proposed that positive regulation of certain promoters in response to ppGpp could occur by an indirect, passive mechanism in which RNA polymerase is limiting and decreased transcription of the strong rRNA promoters in response to ppGpp makes RNA polymerase available for transcription of other promoters (27, 28). The model of indirect stimulation was tested by Choy in a coupled *in vitro* transcription-translation system using positively (*hisp1*) and negatively (*leuVP*) regulated promoters (66). Mixed template and titration experiments demonstrated that there was no inverse correlation between *hisp1* activation and *leuVP* repression under conditions where RNA polymerase amount was made limiting. Furthermore, the extracts seemed to contain titratable factors that could become limiting for promoter stimulation or repression. Together, these results strongly suggested that in the extract system using supercoiled DNA templates, ppGpp-dependent activation and repression are independent, which does not support the passive model of *his* metabolic control (66).

Advances in understanding auxiliary factors and subunits used by RNA polymerase prompted Gourse and coworkers to reprise experiments on the effects of ppGpp on *in vitro* transcription from *hisp1* (175). They showed that ppGpp can indeed significantly increase transcription from the *hisp1* promoter when the potentiator factor DksA is added to the reaction mixtures containing purified RNA polymerase. Other factors, such as the omega subunit of RNA polymerase, also are important for proper function of ppGpp in purified *in vitro* transcription systems (220). Consistent with the *in vitro* transcription results, a Δ*dksA* mutant did not show stimulation of *his* operon transcription following amino acid limitation that increase ppGpp levels (175). Kinetic analyses suggest that the synergistic positive effect of ppGpp and DksA on the transcription at some promoters, such *hisp1*, may occur by

increasing the rate at which RNA polymerase isomerizes to an open complex. Together, these combined results show that ppGpp positively stimulates transcription from the *hisp1* promoter by a direct mechanism, although indirect effects of RNA polymerase concentration might still contribute to *his* metabolic control (175).

Attenuation Control—Histidine-specific and supercoiling-responsive control of *his* operon expression in *E. coli* and *S. typhimurium* is exerted through an attenuation mechanism. The analysis of mutations indicates that attenuation can potentially regulate *his* operon expression over a ≈200-fold range (42, 83, 127). Therefore, the combination of metabolic regulation (≈30-fold) and attenuation (≈200-fold) gives a rather extraordinary total potential range of 6,000 for *his* operon regulation. The discovery of *his* operon attenuation paralleled the work of Yanofsky and his associates on *trp* operon attenuation (see Chapter XX), and results from the two systems led to a rapid elucidation of the mechanism underlying attenuation. Histories of the discovery of *his* operon attenuation were published previously (25, 34). To avoid redundancy with other chapters on attenuation, only the specific aspects of *his* operon attenuation are presented here.

Model for his attenuation—The attenuation model proposes that transcription termination at the *his* attenuator is modulated by synthesis of a peptide encoded by the *his* leader region (29, 30, 34, 59, 78, 126, 127, 132). Except for details, the mechanisms that bring about the coupling of transcription termination and translation are formally similar for *his* and *trp* attenuation. The *his* mechanism relies on two critical features of the *his* leader transcript, which precedes the start of the *hisG* coding region (Fig. 3). First, the *his* leader transcript encodes a 16-amino-acid peptide that contains seven consecutive histidine residues. The paper by Barnes reporting that the *his* leader peptide contains seven tandem histidines (29) had considerable impact, because it dramatically confirmed the generality of the attenuation hypothesis proposed by Lee and Yanofsky (144). Second, a series of mutually exclusive, alternative secondary structures can form in the *his* leader transcript (Fig. 3 and 4). These stem-and-loop structures are formed by pairing between bases in segments A′ and B′, A and B, B and C, C and D, D and E, and E and F in the *his* leader transcript and are designated as A′A:B′B, B:C, C:D, D:E, and E:F, respectively (Fig. 3 and 4). Secondary structure E:F together with the polyuridylate residues downstream from it constitutes a strong Rho factor-independent terminator. If E:F forms, transcription termination occurs at one of the uridylate residues and produces a terminated leader transcript (Fig. 3, Fig. 4, and Table 3). In essence, control by attenuation amounts to varying the frequency at which the E:F terminator structure forms. Any factor, condition, or mutation that prevents E:F terminator formation acts as an antiterminator and allows an RNA polymerase molecule to continue transcription into the *his* operon structural genes. In wild-type attenuation, the antiterminator is an alternative RNA secondary structure D:E (Fig. 4) whose frequency of formation is determined by translation of the leader transcript.

Translation of the *his* leader transcript and formation of alternative secondary structures that signal transcription antitermination or termination are synchronized by pausing of RNA polymerase after formation of the A:B perfect stem-loop structure (Fig. 3 and 4) (57-60, 143). Formation of the upper A:B hairpin is part of the pause signal, and most of RNA

segment B′ probably remains base paired to the DNA template (59, 60, 143). In addition, extending the perfect A:B hairpin by one G:C bp reduces pausing, possibly by interfering with an interaction between the hairpin and RNA polymerase (60). Landick and co-workers have used the *his* pause site as the primary model to dissect the mechanism of transcription pausing (reviewed in (141)). Studies of the *his* pause site have led to the model of the elemental pause state, which involves an off-line rearrangement of the active-site of RNA polymerase that prevents nucleotide substrate addition and does not involve translocation (see (141, 214)). The *his* elemental pause is further stabilized by a multipartite signal that includes the A:B RNA hairpin, which is spaced 2-3 nt from the RNA:DNA hybrid, sequences in the DNA downstream from the pause site in the RNA polymerase active site and sequences in the RNA:DNA hybrid itself (57, 60, 141, 214) Using a combination of biochemical approaches, including single-molecule studies, crosslinking, chemical probing of complexes, and analyses of specific mutations, Landick and co-workers have recently proposed a model for the rearrangements in the active site of RNA polymerase that lead to formation of the elemental pause state and its stabilization by the signals listed above (214). In this model, the “trigger loop” in the active site of RNA polymerase plays roles in NTP loading, translocation, and catalysis during elongation. During pausing, the trigger loop is rearranged to fray the RNA 3’ template away from the DNA template (214). Finally, the *in vitro* half-life of paused RNA polymerase in the *his* leader is unaffected by ppGpp addition and is moderately increased by NusA protein, although no boxA motif is present in or near the A:B structure (59). Enhanced pausing in response to NusA protein seems to require the signals in the *his* leader transcript, including the A:B pause hairpin, but not the downstream DNA signal (59). Whether NusA affects pausing *in vivo* has not been reported.

To see how the attenuation mechanism works *in vivo*, consider bacteria growing in minimal-glucose medium containing histidine. Under these growth conditions, the intracellular concentration of histidine will approach 100 μM, and about 90% of the $tRNA^{His}$ molecules will be charged with histidine (Table 2). An RNA polymerase molecule that initiates transcription at the *hisp1* promoter will start to transcribe the *his* leader region (Fig. 3). A transcribing RNA polymerase molecule will pause at position 102 in the leader transcript partly as a result of A:B hairpin formation (Fig. 4C). Meanwhile, a ribosome will begin to translate the leader transcript and produce the leader peptide. Because the intracellular concentration of His-$tRNA^{His}$ is high, the entire leader peptide will be synthesized, and the translating ribosome will move all the way to the stop codon at position 80 in the transcript. Ribosome movement to this position will disrupt A:B, thereby releasing the RNA polymerase molecule from its paused state, and will mask segments B and B′ in the transcript. When transcription resumes, structure C:D will have an opportunity to form first, preclude formation of structure D:E, and allow the E:F terminator to form (Fig. 4A). Once transcription termination occurs, the RNA polymerase and terminated leader transcript are released spontaneously from the DNA template.

If the translating ribosome rapidly dissociates from the stop codon, A′A:B′B will have an opportunity to form, prevent structure B:C formation, and still allow C:D and E:F to form (Fig. 4C). On the other hand, rapid dissociation of the ribosome at the instant the RNA polymerase molecule is released from pausing could allow synthesis of segment C before A

′A:B′B has a chance to form. This situation would allow B:C formation, which will lead to readthrough transcription. B:C might also have a chance to form by re-equilibration of secondary structures if the transcribing RNA polymerase molecule pauses again in response to C:D formation. However, pausing was detected in a purified *in vitro* transcription system only after A:B hairpin synthesis (59, 143). In either instance, rapid release of ribosomes at the stop codon could account for the relatively high basal level of *his* operon expression detected *in vivo* in the presence of histidine.

Consider next bacteria moderately starved for histidine. Omission of histidine from minimal-glucose medium does not reduce the concentration of His-tRNA^{His} sufficiently (≈80% charged; Table 2) to cause significant read through of the wild-type *his* attenuator. However, mild histidine starvation can be induced genetically (e.g., reference (25)) or by adding the analog 3-amino-1,2,4-triazole (AT), which inhibits one of the HisB enzyme activities (Table 1). Under these conditions, a ribosome translating the leader transcript will stall at the tandem histidine codons, because the cellular concentration of His-tRNA^{His} is low (≤ 12% charged [112]). If a ribosome prevents secondary structure formation in a transcript for about 16 nt downstream from a codon in the aminoacyl site (25, 127), then ribosome stalling at histidine codons 3 to 5 will mask segments A and A′ and release the RNA polymerase molecule from its paused state. Segment C will then be synthesized, and subsequent B:C formation will preclude C:D formation, allow the antiterminator D:E to form, and allow transcription to continue past the *his* attenuator (Fig. 4B).

Antitermination can also be caused by reducing the concentration of His-tRNA^{His} molecules by decreasing the total cellular content of tRNA^{His} molecules (90, 146, 169, 187). In wild-type cells, changes in the absolute cellular concentration of tRNA^{His} molecules may be brought about by modulating the expression of *hisR*, the structural gene for tRNA^{His} (see below). Physiological conditions (e.g., aerobiosis or low osmolarity), antibiotics (e.g., novobiocin), or mutations (e.g., *gyrA* (*hisW*) or *gyrB* [*hisU(I)*]) that decrease negative chromosomal supercoiling are thought to reduce *hisR* expression. This, in turn, reduces the total cellular concentration of tRNA^{His} molecules, thereby decreasing the amount of His-tRNA^{His} and leading to increased *his* operon expression by readthrough of the *his* attenuator (90, 146, 169, 188). In contrast to control by histidine, regulation of *his* operon attenuation by supercoiling should be adaptive and slow, because changes in the total cellular content of tRNA^{His} molecules would require turnover or dilution of stable tRNA molecules by cell growth and division. Finally, if translation of the leader peptide is prevented by a mutation in the initiation codon, super-attenuation occurs. An RNA polymerase molecule transcribes the leader region, pauses after formation of A:B, eventually resumes transcription without assistance from a ribosome, and synthesizes segment C and then segment D of the leader transcript. Formation of C:D prevents D:E formation as the RNA polymerase molecule continues transcription, and the absence of D:E allows formation of the E:F terminator. Super-attenuation should also occur if a translating ribosome stalls upstream of the third histidine codon in the leader transcript, because a ribosome stalled so far upstream in the leader transcript will fail to disrupt A′A:B′B formation (Fig. 4C). It has been reported that *in vivo* attenuator-dependent *his* operon expression is less during severe histidine starvation than during mild histidine starvation (46). This observation can be explained by super-

attenuation which results from occasional stalling of ribosomes at the first two histidine codons in response to severe histidine limitation (25).

Evidence and recent developments—The following features have been well established experimentally for the model of *his* attenuation: (i) response to the intracellular amount of His-tRNA^{His} rather than free histidine (146); (ii) nearly complete evolutionary conservation of the DNA sequence of the *his* leader regions of *E. coli* and *S. typhimurium* (126); (iii) existence of *his* terminated leader and *his* readthrough transcripts *in vivo* and *in vitro* (59, 99, 100, 132); (iv) formation of mutually exclusive, alternative RNA secondary structures in the *his* leader transcript (30, 34, 59, 83, 126, 127, 143); (v) translation of the *his* leader to form the encoded peptide (24, 25, 126, 127); (vi) masking of transcript segments by stalled ribosomes (25, 127); (vii) lack of function of the leader peptide other than to be translated as part of the attenuation mechanism (127); (viii) transcriptional pausing *in vitro* after A:B synthesis (57-60, 141, 143, 214); and (ix) the structure of the paused RNA polymerase complex following A:B synthesis (see (141, 214)).

Some of the most innovative work done on *his* attenuation since the last version of this review concerns the mechanism of pausing (see above). The setting of basal levels of *his* attenuation by rapid release of ribosomes and spontaneous release of the termination complex at the *his* attenuator are based on the model for *trp* attenuation (see Chapter XX) and have not been experimentally verified for *his* attenuation. A recent probabilistic model for attenuation predicts that attenuation is hypersensitive to changes in amino acid supply because of the synchronized start of this mechanism and the small frequencies of usage of the regulatory codons that encode leader peptides (82). The model predicts high basal expression and low sensitivity for the *trp* attenuator and large dynamic range and high sensitivity for *his* attenuation, which includes extra stem- loop structures in the *his* leader compared to the *trp* leader (Fig. 4). However, this model assumes that the basal level of *his* expression is low, which does not match the experimentally results described above. Nevertheless, this model suggests how the extra stem-loop structures in the *his* attenuator might influence the frequency of attenuation (82).

One issue that has been partially resolved is the postulated role of the HisG enzyme as a regulator of *his* operon expression. Suggestive results from a number of experimental approaches led to the conclusion that the HisG enzyme, which binds histidine and His-tRNA^{His} molecules, acts as an autogenous corepressor of *his* operon expression (157). Although this conclusion was instrumental in the formulation of the model of autogenous regulation (104), subsequent genetic and physiological experiments showed conclusively that HisG protein is not an essential component of the mechanism for *his* operon regulation (192). Therefore, the only known forms of *his* operon control are metabolic regulation and attenuation. Results from physiological experiments that implicated HisG protein as a putative corepressor probably reflect indirect effects on intracellular PRPP, ppGpp, or His-tRNA^{His} concentrations. Nevertheless, the HisG enzyme may play a direct but ancillary role in controlling *his* attenuation by acting as a regulated reservoir for His-tRNA^{His} molecules (135). It has also been noted, but not experimentally verified, that the *his* leader transcript has the potential to fold into a cloverleaf secondary structure that resembles the folded tRNA^{His} molecule (14), and this folded *his* leader might bind HisG or other proteins. The

question of whether the HisG enzyme plays some auxiliary role in *his* operon regulation remains unanswered and still needs to be readdressed experimentally.

Role of the his Regulatory Loci

One of the early schemes devised for the selection of *S. typhimurium* mutants with high *his* operon expression relied on resistance to a combination of the analogs AT and 1,2,4-triazole-3-alanine (TRA) (185). AT inhibits the HisB dehydratase activity (Table 1) and reduces histidine biosynthesis, whereas TRA is mistaken for histidine in the cell and is charged onto $tRNA^{His}$ and incorporated into proteins. Growth of wild-type cells is inhibited by a combination of analogs, because AT causes reduction of the histidine supply below a critical level and TRA incorporation presumably inactivates proteins. High expression of the *his* operon caused by mutations can overcome the effect of the analogs and allow the mutant bacteria to grow. Because the absolute amount of His-$tRNA^{His}$ controls the level of *his* attenuation, mutants containing defects in $tRNA^{His}$ biosynthesis were selected by resistance to a combination of AT and TRA. The genes affected in these mutants include: *hisR* (structural gene for $tRNA^{His}$), *gyrA* (*hisW*) and *gyrB* (hisU(I)) (subunits of DNA gyrase), *hisS* (aminoacylation of $tRNA^{His}$ with histidine), *truA* (*hisT*) (pseudouridine modification of the anticocodon stem-loop of $tRNA^{His}$), and *rnpA* (*hisU(II)*) (RNaseP) (processing of $tRNA^{His}$ and the *his* mRNA transcript). Accounting for the high *his* operon expression in these mutants played an important role in working out the mechanism of attenuation control. It was also found that *relA* mutants, which are deficient in ppGpp biosynthesis, are sensitive to AT, and *spoT* mutations, which are defective in ppGpp breakdown, suppress the AT sensitivity of *relA* mutants (186). Moreover, *spoT* mutants, which contain increased ppGpp levels, were found to be resistant to TRA and low concentrations of AT, provided that amino acids other than histidine were added to minimal-glucose media (186).

Genetic schemes were also developed to select for decreases in high-level *his* operon expression. Selection for decreased *his* operon expression has been particularly useful in locating suppressors of mutations in the *his* regulatory loci (e.g., see reference (90). These schemes rely on the complicated phenotypes caused by increased *his* operon expression, including changes in colony morphology and growth inhibition by temperature, adenine, or high salt (90). As mentioned above, some of these phenotypes may be partially attributable to overexpression of the HisH and HisF proteins (163); however, in most cases, the phenotypes remain incompletely understood.

It is beyond the scope of this chapter to describe in detail the molecular genetics of each *his* regulatory locus; however, some features of the *his* regulatory loci that are relevant or unique to the topic of histidine biosynthesis are described. Additional information about the *his* regulatory loci and *relA*, *relC*, and *spoT* is found in other chapters.

hisR—The *hisR* gene codes for the single cellular species of $tRNA^{His}$ in *E. coli* and *S. typhimurium* (37, 42, 126). The $tRNA^{His}$ molecule is unique among tRNAs in that it contains one additional 5′-end nucleotide, which is critical for aminoacylation (118). The single-copy *hisR* gene is part of a tRNA gene cluster whose order is $tRNA^{Arg}$ $tRNA^{His}$-$tRNA^{Leu}$-$tRNA^{Pro}$ in both *E. coli* and *S. typhimurium* (37, 121). Recently, it was shown that

the RNaseE endonuclease acts to process the precursor transcript that contains $tRNA^{Arg}$-$tRNA^{His}$-$tRNA^{Leu}$-$tRNA^{Pro}$ (172) This cleavage by RNaseE precedes processing by RNaseP and 3' → 5' exonucleases and accounts for the reason that RNaseE activity is essential for cell viability (172). The genes in the $tRNA^{Arg}$-$tRNA^{His}$ $tRNA^{Leu}$-$tRNA^{Pro}$ operon are bounded by a promoter, which has an upstream activating sequences in its -70 region, a stringency-control discriminator sequence between the -10 region and the start point of transcription, and a Rho-independent terminator (37, 38, 121).

Mutations in the *S. typhimurium hisR* promoter reduce the total cellular content of $tRNA^{His}$ molecules by about 50% and thereby cause increased read-through transcription of the *his* attenuator (38). Likewise, mutations or antibiotics that decrease negative supercoiling, such as in *gyrAB* or quinolone-family antibiotics, reduce expression of the *hisR* promoter, which leads to decreased cellular amounts of $HistRNA^{His}$, increased read-through of the *his* attenuator, and increased *his* operon expression (42, 72, 89, 90, 187). As noted above, this effect of supercoiling is restricted to *his* attenuation rather than on transcription from the *hisp1* promoter (169), even though transcription from *hisp1* does depend on supercoiling in an *in vitro* coupled transcription-translation system (184). Consistent with this conclusion, normal *his* operon expression is restored in a gyrA (*hisW*) mutant by an episome carrying a single copy of the *hisR* gene (42). The dependence of the *hisR* promoter on supercoiling seems to depend, in part, on the stringency discriminator sequence (89, 90). Another interesting recent finding is that temperature-sensitive *dnaA* mutants show increased read-through of the *his* attenuator and increased *his* operon expression when grown in rich media (33). This effect is suppressed by simply increasing the copy number of *hisR.* In this case, an imbalance between the gene dosage may occur between the *hisR* locus, which is close to *oriC*, and the *his* operon, which is far from *oriC*, leading to a decrease in the *hisR* to *his* operon gene ratio (33).

hisS—The *hisS* gene encodes histidyl-tRNA synthetase (HisRS), which aminoacylates $tRNA^{His}$ molecules with histidine (Table 1). The histidyl-tRNA synthetase is a class II synthetase (188). Francklyn and coworkers have determined the structure of HisRS bound to several substrates and amino acid analogues (see (96)). They have also used HisRS as a model to study the mechanism of aminoacylation of a class II synthetase and the basis of the discrimination between cognate and noncognate tRNA substrates (see (110)). Because attenuation responds to the amount of $His\text{-}tRNA^{His}$, the activity of the histidyl-tRNA synthetase affects histidine biosynthesis. In wild-type cells growing in minimal-glucose medium without histidine, the K_m of histidyl-tRNA synthetase for histidine is comparable to the histidine concentration (Tables 1 and 2). In this concentration range, the rate of aminoacylation should be strongly affected by fluctuations in the histidine concentration (42). In addition, aminoacylation of $tRNA^{His}$ is noncompetitively inhibited by AMP (77), competitively inhibited by ADP or adenosine (77), very strongly inhibited by AMP in the presence of pyrophosphate (44), and strongly product inhibited by $His\text{-}tRNA_{His}$ (44). This pattern of inhibition has three consequences that could affect the intracellular amount of $His\text{-}tRNA^{His}$ and thereby influence the rate of histidine biosynthesis: (i) the activity of histidyl-tRNA synthetase is subject to control by cellular energy charge, like the HisG enzyme (see above and reference (43)); (ii) product inhibition probably plays a role in setting the

percentage of $tRNA^{His}$ molecules that are charged at a given histidine concentration (146); and (iii) only a small fraction of the His-tRNA synthetase molecules will be active in bacteria growing under normal conditions because of product inhibition by the high percentage of charged $tRNA^{His}$ molecules (Table 2 and reference (44)).

Mutations in the *hisS* gene that affect the level of *his* attenuation act by reducing the percentage of $tRNA^{His}$ molecules charged with histidine (146). These mutations generally lower the catalytic activity of HisRS or decrease the affinity of HisRS for histidine, $tRNA_{His}$, or ATP (75). This conclusion was confirmed by recent detailed biochemical analysis of five of these earlier *hisS* mutants (96). Furthermore, histidine biosynthesis seems to be linked directly to the control of the *hisS* gene, since limitation for histidine causes increased expression of *hisS in vivo* (156). However, the regulation of *hisS* is not well understood.

truA) hisT—The *truA* (*hisT*) gene encodes PSUI, which catalyzes formation of pseudouridine residues at positions 38, 39, and 40 in the anti-codon stem and loop of at least 30 tRNA isoaccepting species, including $tRNA^{His}$ (Table 1) (196, 216). The structure of the PSUI homodimer was recently reported unbound and bound to tRNA (94, 124), and the ability of PSUI to modify three different position in different tRNA molecules was studied by combining the structural studies with kinetic studies and computer simulations (124). Transcription termination at the *his* attenuator is greatly decreased in *truA* (*hisT*) mutants even though the undermodified $tRNA^{His}$ molecules are charged with histidine to the same extent as in wild-type strains (148). To explain this observation, it was postulated that undermodification of His-$tRNA^{His}$ molecules in *truA* (*hisT*) mutants slows translation of the seven histidine codons contained in the *his* leader transcript and thereby mimics ribosome stalling induced by low concentrations of His-$tRNA^{His}$ in wild-type bacteria moderately starved for histidine (126). Slow translation or ribosome stalling will result in increased transcription read-through of the *his* attenuator (Fig. 4B). Support for this conjecture has come from kinetic experiments which show that the absence of pseudouridine modifications in *truA* (*hisT*) mutants reduces the general rate of translation elongation by at least 25% and severely reduces translation of mRNA molecules and leader transcripts containing runs of codons for the same amino acid (23, 173). In addition, in some codon contexts, *truA* (*hisT*)-mediated tRNA modification is important for reading frame maintenance during translation (217).

Starvation for amino acids results in preferential undermodification for pseudouridine residues at positions 38, 39, and 40 in tRNA molecules in some genetic backgrounds (133, 212). This tRNA undermodification parallels the effect of the *truA* (*hisT*) mutation and may lead to increased *his* operon expression in response to general amino acid deprivation, although further study is needed. A related issue concerns the possibility that histidine biosynthesis is affected by fluctuations in the level of expression of the *truA* (*hisT*) gene itself. The *truA* (*hisT*) gene is in a complex superoperon with at least three other genes, including the *pdxB* gene required for the biosynthesis of the essential coenzyme, pyridoxal 5′-phosphate (21, 22, 155). *truA* (*hisT*) expression is positively regulated by growth rate in a way that would coordinate the amounts of PSUI and tRNA molecules (215). PSUI amounts may also be regulated by translational coupling to the expression of an upstream

dehydrogenase gene (22, 155). The number of PSUI molecules in the cell seems limited (131), and so parallel regulation of PSUI and tRNA amounts may be important for maintaining full tRNA modification levels.

HISTIDINE TRANSPORT

Histidine uptake and its regulation is reviewed elsewhere (see Chapter XX), but there are a couple of considerations about uptake that impact histidine biosynthesis. Histidine can enter *Salmonella typhimurium* by at least five uptake system ((12); Chapter XX on Amino Acid Utilization), including the high-affinity histidine periplasmic-binding-protein (HisJ-HisQ-HisM-HisP) system (Table 2). The histidine periplasmic-binding-protein permease has been studied extensively by G. F. Ames and coworkers (see references (15, 18, 79, 149, 168) and is one of the best characterized ABC ATP-dependent transport systems (see Chapter XX). The K_m of the HisJ-HisQ-HisM-HisP permease for histidine is about 10^{-8} M and the K_d (histidine) of the HisJ periplasmic binding protein is about 0.1 μM, which means that its affinity for histidine is orders of magnitude greater than that of some of the other histidine transport systems (12); Chapter XX). The HisJ-HisQ-HisM-HisP permease can concentrate histidine against a very high concentration gradient and scavenge histidine at very low concentrations (15, 17, 79). The *S. typhimurium* histidine limit concentration, which is the lowest external concentration required by the HisJ-HisQ-HisM-HisP permease to supply the cell with enough histidine for protein synthesis without endogenous histidine biosynthesis, is only 0.15 μM (Table 2) (12, 15). It has been suggested that bacterial cells need to maintain such an efficient and complex histidine permease because there is a certain amount of leakage of histidine from bacterial cells (15, 17, 79). Since the biosynthesis of each histidine molecule requires so much energy (see above), it may be advantageous for bacteria to recover any histidine lost to the growth medium. It has also been pointed out that the high affinity of amino acid permeases makes bioassays possible (15). Finally, the high affinity of the HisJ-HisQ-HisM-HisP permease may explain why bacterial cells need to maintain high basal concentrations of the histidine biosynthetic enzymes even in the presence of exogenous histidine (Table 2) (42). Since transport of histidine is so effective at low concentrations, the internal pool of histidine will not decrease significantly until the external histidine supply is almost completely gone. If attenuation greatly lowered the amounts of the histidine biosynthetic enzymes in response to external histidine supply, then it is conceivable that there would not be enough time for adequate transcription and translation of the *his* structural genes between when the internal histidine pool starts to fall and when the total histidine supply is exhausted. Hence, a system may have evolved that favors histidine transport at the relatively small energy expense of maintaining a constant supply of the histidine biosynthetic enzymes (42).

SUMMARY

In all major respects, histidine biosynthesis seems to be the same in *E. coli* and *S. typhimurium*. Histidine biosynthesis in *E. coli* and *S. typhimurium* has continued to provide a wealth of fundamental information about biochemical and cellular regulation that go far beyond the topic of histidine biosynthesis. Some of these advances are highlighted in this review, including insights into the mechanisms of allosteric feedback inhibition, cooperative

control of enzyme function, unique enzymatic reactions, positive metabolic control by ppGpp, pausing of RNA polymerase, attenuation, and pathway evolution. The progress in these areas will continue as sophisticated genomic, metabolomic, proteomic, and structural approaches converge in studies of the histidine biosynthetic pathway and mechanisms of control of the *his* operon. In addition, the new methods that have emerged recently to construct directed chromosomal mutations efficiently combined with whole-genome methods to identify mutations that arise in selections rapidly at reasonable cost should build on the more classical studies done so far on the physiological consequences of biochemical changes on histidine biosynthesis and *his* operon control.

ACKNOWLEDGMENTS

I thank the many scientists who have worked or continue to work on the biosynthesis of histidine in *E. coli* and *S. typhimurium* for helpful discussions, information, and insights into this topic and Krystyna M. Kazmierczak for comments on the manuscript. Preparation of this review was supported by grants AI060744 from the National Institutes of Health and 0543289 from the National Science Foundation of the U.S.A. to M. E. W., and by funds from the Indiana METACyt Initiative of Indiana University Bloomington, funded in part through a major grant from the Lilly Endowment, Inc. to M.E.W.

This chapter is dedicated to the memory of Philip E. Hartman and Zlata Demerec Hartman (Johns Hopkins University), who were pioneers of bacterial genetics and education, made numerous fundamental discoveries about the *his* operon, bacterial metabolism, and mutagenesis, and were outstanding mentors and role models to many in the field.

LITERATURE CITED

1. Albritton WL, Levin AP. Some comparative kinetic data on the enzyme imidazoleacetol phosphate:L-glutamate aminotransferase derived from mutant strains of *Salmonella typhimurium*. J Biol Chem. 1970; 245:2525–8. [PubMed: 5445798]
2. Alifano P, Carlomagno MS, Bruni CB. Location of the *hisGDCBHAFI* operon on the physical map of *Escherichia coli*. J Bacteriol. 1992; 174:3830–1. [PubMed: 1592835]
3. Alifano P, Ciampi MS, Nappo AG, Bruni CB, Carlomagno MS. *In vivo* analysis of the mechanisms responsible for strong transcriptional polarity in a “sense” mutant within an intercistronic region. Cell. 1988; 55:351–60. [PubMed: 3048706]
4. Alifano P, Fani R, Lio P, Lazcano A, Bazzicalupo M, Carlomagno MS, Bruni CB. Histidine biosynthetic pathway and genes: structure, regulation, and evolution. Microbiol Rev. 1996; 60:44–69. [PubMed: 8852895]
5. Alifano P, Piscitelli C, Blasi V, Rivellini F, Nappo AG, Bruni CB, Carlomagno MS. Processing of a polycistronic mRNA requires a 5′ cis element and active translation. Mol Microbiol. 1992; 6:787–98. [PubMed: 1374148]
6. Alifano P, Rivellini F, Limauro D, Bruni CB, Carlomagno MS. A consensus motif common to all Rho-dependent prokaryotic transcription terminators. Cell. 1991; 64:553–63. [PubMed: 1703923]
7. Alifano P, Rivellini F, Nappo AG, Bruni CB, Carlomagno MS. Alternative patterns of his operon transcription and mRNA processing generated by metabolic perturbation. Gene. 1994; 146:15–21. [PubMed: 8063100]
8. Alifano P, Rivellini F, Piscitelli C, Arraiano CM, Bruni CB, Carlomagno MS. Ribonuclease E provides substrates for ribonuclease P-dependent processing of a polycistronic mRNA. Genes Dev. 1994; 8:3021–31. [PubMed: 8001821]
9. Allen S, Zilles JL, Downs DM. Metabolic flux in both the purine mononucleotide and histidine biosynthetic pathways can influence synthesis of the hydroxymethyl pyrimidine moiety of thiamine in *Salmonella enterica*. J Bacteriol. 2002; 184:6130–7. [PubMed: 12399482]
10. Amaro RE, Myers RS, Davisson VJ, Luthey-Schulten ZA. Structural elements in IGP synthase exclude water to optimize ammonia transfer. Biophys J. 2005; 89:475–87. [PubMed: 15849257]

11. Amaro RE, Sethi A, Myers RS, Davisson VJ, Luthey-Schulten ZA. A network of conserved interactions regulates the allosteric signal in a glutamine amidotransferase. Biochemistry. 2007; 46:2156–73. [PubMed: 17261030]
12. Ames, BN. A bacterial system for detecting mutagens and carcinomas. In: Sutton, HE.; Harris, MI., editors. Mutagenic Effects of Environmental Contaminants. Academic Press, Inc.; New York: 1972. p. 57-66.
13. Ames BN, Durston WE, Yamasaki E, Lee FD. Carcinogens are mutagens: a simple test system combining liver homogenates for activation and bacteria for detection. Proc Natl Acad Sci USA. 1973; 70:2281–5. [PubMed: 4151811]
14. Ames BN, Tsang TH, Buck M, Christman MF. The leader mRNA of the histidine attenuator region resembles tRNAHis: possible general regulatory implications. Proc Natl Acad Sci USA. 1983; 80:5240–2. [PubMed: 6351055]
15. Ames GF. Bacterial periplasmic transport systems: structure, mechanism, and evolution. Annu Rev Biochem. 1986; 55:397–425. [PubMed: 3527048]
16. Ames, GF. Components of histidine transport. In: Fox, CF., editor. Membrane Research. Academic Press, Inc.; New York: 1972. p. 409-426.
17. Ames GF. Uptake of Amino Acids by *Salmonella typhimurium*. Arch Biochem Biophys. 1964; 104:1–18. [PubMed: 14110716]
18. Ames GF, Nikaido K, Wang IX, Liu PQ, Liu CE, Hu C. Purification and characterization of the membrane-bound complex of an ABC transporter, the histidine permease. J Bioenerg Biomembr. 2001; 33:79–92. [PubMed: 11456221]
19. Arnez JG, Augustine JG, Moras D, Francklyn CS. The first step of aminoacylation at the atomic level in histidyl-tRNA synthetase. Proc Natl Acad Sci USA. 1997; 94:7144–9. [PubMed: 9207058]
20. Arnez JG, Harris DC, Mitschler A, Rees B, Francklyn CS, Moras D. Crystal structure of histidyl-tRNA synthetase from *Escherichia coli* complexed with histidyl-adenylate. EMBO J. 1995; 14:4143–55. [PubMed: 7556055]
21. Arps PJ, Marvel CC, Rubin BC, Tolan DA, Penhoet EE, Winkler ME. Structural features of the hisT operon of *Escherichia coli* K-12. Nucleic Acids Res. 1985; 13:5297–315. [PubMed: 2991861]
22. Arps PJ, Winkler ME. An unusual genetic link between vitamin B6 biosynthesis and tRNA pseudouridine modification in Escherichia coli K-12. J Bacteriol. 1987; 169:1071–9. [PubMed: 3029017]
23. Artz S, Holzschu D, Blum P, Shand R. Use of M13mp phages to study gene regulation, structure and function: cloning and recombinational analysis of genes of the *Salmonella typhimurium* histidine operon. Gene. 1983; 26:147–58. [PubMed: 6323256]
24. Artz SW, Broach JR. Histidine regulation in *Salmonella typhimurium*: an activator attenuator model of gene regulation. Proc Natl Acad Sci USA. 1975; 72:3453–7. [PubMed: 1103149]
25. Artz, SW.; Holzschu, D. Histidine biosynthesis and its regulation. In: Herrmann, KM.; Somerville, RL., editors. Amino Acids: Biosynthesis and Genetic Regulation. Addison-Wesley Publishing Co.; Rading, Massachusetts: 1983. p. 379-404.
26. Barbosa JA, Sivaraman J, Li Y, Larocque R, Matte A, Schrag JD, Cygler M. Mechanism of action and NAD^+-binding mode revealed by the crystal structure of L-histidinol dehydrogenase. Proc Natl Acad Sci USA. 2002; 99:1859–64. [PubMed: 11842181]
27. Barker MM, Gaal T, Gourse RL. Mechanism of regulation of transcription initiation by ppGpp. II. Models for positive control based on properties of RNAP mutants and competition for RNAP. J Mol Biol. 2001; 305:689–702. [PubMed: 11162085]
28. Barker MM, Gaal T, Josaitis CA, Gourse RL. Mechanism of regulation of transcription initiation by ppGpp. I. Effects of ppGpp on transcription initiation *in vivo* and *in vitro*. J Mol Biol. 2001; 305:673–88. [PubMed: 11162084]
29. Barnes WM. DNA sequence from the histidine operon control region: seven histidine codons in a row. Proc Natl Acad Sci USA. 1978; 75:4281–5. [PubMed: 360216]
30. Barnes WM, Tuley E. DNA sequence changes of mutations in the histidine operon control region that decrease attenuation. J Mol Biol. 1983; 165:443–59. [PubMed: 6302291]

31. Batchelor RA, Alifano P, Biffali E, Hull SI, Hull RA. Nucleotide sequences of the genes regulating O-polysaccharide antigen chain length (rol) from *Escherichia coli* and *Salmonella typhimurium*: protein homology and functional complementation. J Bacteriol. 1992; 174:5228–36. [PubMed: 1379582]
32. Berberich MA, Kovach JS, Goldberger RF. Chain initiation in a polycistronic message: sequential versus simultaneous derepression of the enzymes for histidine biosynthesis in *Salmonella typhimurium*. Proc Natl Acad Sci USA. 1967; 57:1857–64. [PubMed: 5340637]
33. Blanc-Potard AB, Figueroa-Bossi N, Bossi L. Histidine operon deattenuation in dnaA mutants of *Salmonella typhimurium* correlates with a decrease in the gene dosage ratio between tRNA(His) and histidine biosynthetic loci. J Bacteriol. 1999; 181:2938–41. [PubMed: 10217789]
34. Blasi F, Bruni CB. Regulation of the histidine operon: translation-controlled transcription termination (a mechanism common to several biosynthetic operons). Curr Top Cell Regul. 1981; 19:1–45. [PubMed: 6277571]
35. Bochner BR, Ames BN. Complete analysis of cellular nucleotides by two-dimensional thin layer chromatography. J Biol Chem. 1982; 257:9759–69. [PubMed: 6286632]
36. Bochner BR, Ames BN. ZTP (5-amino 4-imidazole carboxamide riboside 5′-triphosphate): a proposed alarmone for 10-formyl-tetrahydrofolate deficiency. Cell. 1982; 29:929–37. [PubMed: 6185232]
37. Bossi L. The hisR locus of *Salmonella*: nucleotide sequence and expression. Mol Gen Genet. 1983; 192:163–70. [PubMed: 6358794]
38. Bossi L, Smith DM. Conformational change in the DNA associated with an unusual promoter mutation in a tRNA operon of *Salmonella*. Cell. 1984; 39:643–52. [PubMed: 6096016]
39. Bovee ML, Champagne KS, Demeler B, Francklyn CS. The quaternary structure of the HisZ-HisG N-1-(5′-phosphoribosyl)-ATP transferase from *Lactococcus lactis*. Biochemistry. 2002; 41:11838–46. [PubMed: 12269828]
40. Brady DR, Houston LL. New assay for histidinol phosphate phosphatase using a coupled reaction. Anal Biochem. 1972; 48:480–2. [PubMed: 4341769]
41. Brady DR, Houston LL. Some properties of the catalytic sites of imidazoleglycerol phosphate dehydratase-histidinol phosphate phosphatase, a bifunctional enzyme from *Salmonella typhimurium*. J Biol Chem. 1973; 248:2588–92. [PubMed: 4349042]
42. Brenner, M.; Ames, BN. The histidine operon and its regulation. In: Vogel, HJ., editor. Metabolic Pathways. Vol. 5. Academic Press; New York: 1971. p. 349-387.
43. Brenner M, De Lorenzo F, Ames BN. Energy charge and protein synthesis. Control of aminoacyl transfer ribonucleic acid synthetases. J Biol Chem. 1970; 245:450–2. [PubMed: 4904484]
44. Brenner M, Lewis JA, Straus DS, De Lorenzo F, Ames BN. Histidine regulation in *Salmonella typhimurium*. XIV. Interaction of the histidyl transfer ribonucleic acid synthetase with histidine transfer ribonucleic acid. J Biol Chem. 1972; 247:4333–9. [PubMed: 4338485]
45. Brilli M, Fani R. Molecular evolution of hisB genes. J Mol Evol. 2004; 58:225–37. [PubMed: 15042344]
46. Bruni CB, Musti AM, Frunzio R, Blasi F. Structural and physiological studies of the *Escherichia coli* histidine operon inserted into plasmid vectors. J Bacteriol. 1980; 142:32–42. [PubMed: 6246067]
47. Cano DA, Mouslim C, Ayala JA, Garcia-del Portillo F, Casadesus J. Cell division inhibition in *Salmonella typhimurium* histidine-constitutive strains: an ftsI-like defect in the presence of wild-type penicillin-binding protein 3 levels. J Bacteriol. 1998; 180:5231–4. [PubMed: 9748459]
48. Carlomagno MS, Blasi F, Bruni CB. Gene organization in the distal part of the *Salmonella typhimurium* histidine operon and determination and sequence of the operon transcription terminator. Mol Gen Genet. 1983; 191:413–20. [PubMed: 6314092]
49. Carlomagno MS, Chiariotti L, Alifano P, Nappo AG, Bruni CB. Structure and function of the *Salmonella typhimurium* and *Escherichia coli* K-12 histidine operons. J Mol Biol. 1988; 203:585–606. [PubMed: 3062174]
50. Carlomagno MS, Nappo A. The antiterminator NusB enhances termination at a sub-optimal Rho site. J Mol Biol. 2001; 309:19–28. [PubMed: 11491288]

51. Carlomagno MS, Nappo A. NusA modulates intragenic termination by different pathways. Gene. 2003; 308:115–28. [PubMed: 12711396]
52. Carlomagno MS, Riccio A, Bruni CB. Convergently functional, Rho-independent terminator in *Salmonella typhimurium*. J Bacteriol. 1985; 163:362–8. [PubMed: 3891737]
53. Carrano L, Alifano P, Corti E, Bucci C, Donadio S. A new inhibitor of the transcription-termination factor Rho. Biochem Biophys Res Commun. 2003; 302:219–25. [PubMed: 12604334]
54. Carrano L, Bucci C, De Pascalis R, Lavitola A, Manna F, Corti E, Bruni CB, Alifano P. Effects of bicyclomycin on RNA- and ATP-binding activities of transcription termination factor Rho. Antimicrob Agents Chemother. 1998; 42:571–8. [PubMed: 9517934]
55. Cashel, M.; Rudd, KE. Stringent response. In: Neidhardt, FC.; Ingraham, JL.; Low, KB.; Magasanik, B.; Schaechter, M.; Umbarger, HE., editors. *Escherichia coli* and *Salmonella typhimurium*: Cellular and Molecular Biology. American Society for Microbiology; Washington, D.C.: 1987. p. 1410-1438.
56. Champagne KS, Sissler M, Larrabee Y, Doublie S, Francklyn CS. Activation of the hetero-octameric ATP phosphoribosyl transferase through subunit interface rearrangement by a tRNA synthetase paralog. J Biol Chem. 2005; 280:34096–104. [PubMed: 16051603]
57. Chan CL, Landick R. Dissection of the his leader pause site by base substitution reveals a multipartite signal that includes a pause RNA hairpin. J Mol Biol. 1993; 233:25–42. [PubMed: 8377190]
58. Chan CL, Landick R. Effects of neutral salts on RNA chain elongation and pausing by *Escherichia coli* RNA polymerase. J Mol Biol. 1997; 268:37–53. [PubMed: 9149140]
59. Chan CL, Landick R. The *Salmonella typhimurium* his operon leader region contains an RNA hairpin-dependent transcription pause site. Mechanistic implications of the effect on pausing of altered RNA hairpins. J Biol Chem. 1989; 264:20796–804. [PubMed: 2479649]
60. Chan CL, Wang D, Landick R. Multiple interactions stabilize a single paused transcription intermediate in which hairpin to 3′ end spacing distinguishes pause and termination pathways. J Mol Biol. 1997; 268:54–68. [PubMed: 9149141]
61. Chaudhuri BN, Lange SC, Myers RS, Davisson VJ, Smith JL. Toward understanding the mechanism of the complex cyclization reaction catalyzed by imidazole glycerolphosphate synthase: crystal structures of a ternary complex and the free enzyme. Biochemistry. 2003; 42:7003–12. [PubMed: 12795595]
62. Cheong CG, Bauer CB, Brushaber KR, Escalante-Semerena JC, Rayment I. Three-dimensional structure of the L-threonine-O-3-phosphate decarboxylase (CobD) enzyme from *Salmonella enterica*. Biochemistry. 2002; 41:4798–808. [PubMed: 11939774]
63. Cheong CG, Escalante-Semerena JC, Rayment I. Structural studies of the L-threonine-O-3-phosphate decarboxylase (CobD) enzyme from *Salmonella enterica*: the apo, substrate, and product-aldimine complexes. Biochemistry. 2002; 41:9079–89. [PubMed: 12119022]
64. Chittur SV, Klem TJ, Shafer CM, Davisson VJ. Mechanism for acivicin inactivation of triad glutamine amidotransferases. Biochemistry. 2001; 40:876–87. [PubMed: 11170408]
65. Cho Y, Sharma V, Sacchettini JC. Crystal structure of ATP phosphoribosyltransferase from *Mycobacterium tuberculosis*. J Biol Chem. 2003; 278:8333–9. [PubMed: 12511575]
66. Choy HE. The study of guanosine 5′-diphosphate 3′-diphosphate-mediated transcription regulation *in vitro* using a coupled transcription-translation system. J Biol Chem. 2000; 275:6783–9. [PubMed: 10702235]
67. Ciesla Z, Salvatore F, Broach JR, Artz SW, Ames BN. Histidine regulation in *Salmonella typhimurium*. XVI. A sensitive radiochemical assay for histidinol dehydrogenase. Anal Biochem. 1975; 63:44–55. [PubMed: 1089301]
68. Cortese R, Kammen HO, Spengler SJ, Ames BN. Biosynthesis of pseudouridine in transfer ribonucleic acid. J Biol Chem. 1974; 249:1103–8. [PubMed: 4592259]
69. D'Ordine RL, Klem TJ, Davisson VJ. N1-(5′-phosphoribosyl) adenosine-5′-monophosphate cyclohydrolase: purification and characterization of a unique metalloenzyme. Biochemistry. 1999; 38:1537–46. [PubMed: 9931020]

70. Da Costa XJ, Artz SW. Mutations that render the promoter of the histidine operon of *Salmonella typhimurium* insensitive to nutrient-rich medium repression and amino acid downshift. J Bacteriol. 1997; 179:5211–7. [PubMed: 9260966]
71. Dall-Larsen T. Stopped flow kinetic studies of adenosine triphosphate phosphoribosyl transferase, the first enzyme in the histidine biosynthesis of *Escherichia coli*. Int J Biochem. 1988; 20:811–5. [PubMed: 3049184]
72. Davis L, Williams LS. Characterization of a cold-sensitive hisW mutant of *Salmonella typhimurium*. J Bacteriol. 1982; 151:867–78. [PubMed: 6178723]
73. De Lorenzo F, Ames BN. Histidine regulation in *Salmonella typhimurium*. VII. Purification and general properties of the histidyl transfer ribonucleic acid synthetase. J Biol Chem. 1970; 245:1710–6. [PubMed: 4985616]
74. De Lorenzo F, Di Natale P, Schechter AN. Chemical and physical studies on the structure of the histidyl transfer ribonucleic acid synthetase from *Salmonella typhimurium*. J Biol Chem. 1974; 249:908–13. [PubMed: 4590693]
75. De Lorenzo F, Straus DS, Ames BN. Histidine regulation in *Salmonella typhimurium*. X. Kinetic studies of mutant histidyl transfer ribonucleic acid synthetases. J Biol Chem. 1972; 247:2302–7. [PubMed: 4553439]
76. Di Natale P, Cimino F, De Lorenzo F. The pyrophosphate exchange reaction of histidyl-tRNA synthetase from *Salmonella typhimurium*: reaction parameters and inhibition by transfer ribonucleic acid. FEBS Lett. 1974; 46:175–9. [PubMed: 4371484]
77. Di Natale P, Schechter AN, Castronuovo Lepore G, De Lorenzo F. Histidyl transfer ribonucleic acid synthetase from *Salmonella typhimurium*. Interaction with substrates and ATP analogues. Eur J Biochem. 1976; 62:293–8. [PubMed: 3414]
78. Di Nocera PP, Blasi F, Di Lauro R, Frunzio R, Bruni CB. Nucleotide sequence of the attenuator region of the histidine operon of *Escherichia coli* K-12. Proc Natl Acad Sci USA. 1978; 75:4276–80. [PubMed: 360215]
79. Doige CA, Ames GF. ATP-dependent transport systems in bacteria and humans: relevance to cystic fibrosis and multidrug resistance. Annu Rev Microbiol. 1993; 47:291–319. [PubMed: 7504904]
80. Douangamath A, Walker M, Beismann-Driemeyer S, Vega-Fernandez MC, Sterner R, Wilmanns M. Structural evidence for ammonia tunneling across the (beta alpha)(8) barrel of the imidazole glycerol phosphate synthase bienzyme complex. Structure. 2002; 10:185–93. [PubMed: 11839304]
81. Durfee T, Hansen AM, Zhi H, Blattner FR, Jin DJ. Transcription profiling of the stringent response in *Escherichia coli*. J Bacteriol. 2008; 190:1084–96. [PubMed: 18039766]
82. Elf J, Ehrenberg M. What makes ribosome-mediated transcriptional attenuation sensitive to amino acid limitation? PLoS Comput Biol. 2005; 1:e2. [PubMed: 16103903]
83. Ely B. Physiological studies of *Salmonella* histidine operator-promoter mutants. Genetics. 1974; 78:593–606. [PubMed: 4375069]
84. Ely B, Ciesla Z. Internal promoter P2 of the histidine operon of *Salmonella typhimurium*. J Bacteriol. 1974; 120:984–6. [PubMed: 4616955]
85. Fani R, Brilli M, Fondi M, Lio P. The role of gene fusions in the evolution of metabolic pathways: the histidine biosynthesis case. BMC Evol Biol 7 Suppl. 2007; 2:S4.
86. Fani R, Brilli M, Lio P. The origin and evolution of operons: the piecewise building of the proteobacterial histidine operon. J Mol Evol. 2005; 60:378–90. [PubMed: 15871048]
87. Fani R, Mori E, Tamburini E, Lazcano A. Evolution of the structure and chromosomal distribution of histidine biosynthetic genes. Orig Life Evol Biosph. 1998; 28:555–70. [PubMed: 9742729]
88. Fernandez FJ, Vega MC, Lehmann F, Sandmeier E, Gehring H, Christen P, Wilmanns M. Structural studies of the catalytic reaction pathway of a hyperthermophilic histidinol-phosphate aminotransferase. J Biol Chem. 2004; 279:21478–88. [PubMed: 15007066]
89. Figueroa-Bossi N, Guerin M, Rahmouni R, Leng M, Bossi L. The supercoiling sensitivity of a bacterial tRNA promoter parallels its responsiveness to stringent control. Embo J. 1998; 17:2359–67. [PubMed: 9550733]
90. Figueroa N, Wills N, Bossi L. Common sequence determinants of the response of a prokaryotic promoter to DNA bending and supercoiling. Embo J. 1991; 10:941–9. [PubMed: 1849077]

91. Fink GR, Martin RG. Translation and polarity in the histidine operon. II. Polarity in the histidine operon. J Mol Biol. 1967; 30:97–107. [PubMed: 4294872]
92. Fishman SE, Kerchief KR, Parker J. Specialized lambda transducing bacteriophage which carries hisS, the structural gene for histidyl-transfer ribonucleic acid synthetase. J Bacteriol. 1979; 139:404–10. [PubMed: 378969]
93. Flores A, Fox M, Casadesus J. The pleiotropic effects of his overexpression in *Salmonella typhimurium* do not involve AICAR-induced mutagenesis. Mol Gen Genet. 1993; 240:360–4. [PubMed: 8413185]
94. Foster PG, Huang L, Santi DV, Stroud RM. The structural basis for tRNA recognition and pseudouridine formation by pseudouridine synthase I. Nat Struct Biol. 2000; 7:23–7. [PubMed: 10625422]
95. Fox M, Frandsen N, D'Ari R. AICAR is not an endogenous mutagen in *Escherichia coli*. Mol Gen Genet. 1993; 240:355–9. [PubMed: 8413184]
96. Francklyn C, Adams J, Augustine J. Catalytic defects in mutants of class II histidyl-tRNA synthetase from *Salmonella typhimurium* previously linked to decreased control of histidine biosynthesis regulation. J Mol Biol. 1998; 280:847–58. [PubMed: 9671554]
97. Francklyn C, Schimmel P. Enzymatic aminoacylation of an eight-base-pair microhelix with histidine. Proc Natl Acad Sci USA. 1990; 87:8655–9. [PubMed: 2236077]
98. Frandsen N, D'Ari R. Excess histidine enzymes cause AICAR-independent filamentation in *Escherichia coli*. Mol Gen Genet. 1993; 240:348–54. [PubMed: 8413183]
99. Freedman R, Schimmel P. *In vitro* transcription of the histidine operon. Identification of the *his* promoter and leader and readthrough transcripts. J Biol Chem. 1981; 256:10747–50. [PubMed: 6270128]
100. Frunzio R, Bruni CB, Blasi F. *In vivo* and *in vitro* detection of the leader RNA of the histidine operon of *Escherichia coli* K-12. Proc Natl Acad Sci USA. 1981; 78:2767–71. [PubMed: 6166940]
101. Gee P, Maron DM, Ames BN. Detection and classification of mutagens: a set of base-specific *Salmonella* tester strains. Proc Natl Acad Sci USA. 1994; 91:11606–10. [PubMed: 7972111]
102. Gibert I, Casadesus J. *sulA*-independent division inhibition in his-constitutive strains of *Salmonella typhimurium*. FEMS Microbiol Lett. 1990; 57:205–10. [PubMed: 2210331]
103. Glynn SE, Baker PJ, Sedelnikova SE, Davies CL, Eadsforth TC, Levy CW, Rodgers HF, Blackburn GM, Hawkes TR, Viner R, Rice DW. Structure and mechanism of imidazoleglycerol-phosphate dehydratase. Structure. 2005; 13:1809–17. [PubMed: 16338409]
104. Goldberger RF. Autogenous regulation of gene expression. Science. 1974; 183:810–6. [PubMed: 4589900]
105. Grisolia V, Carlomagno MS, Nappo AG, Bruni CB. Cloning, structure, and expression of the *Escherichia coli* K-12 hisC gene. J Bacteriol. 1985; 164:1317–23. [PubMed: 2999081]
106. Grisolia V, Riccio A, Bruni CB. Structure and function of the internal promoter (*hisBp*) of the *Escherichia coli* K-12 histidine operon. J Bacteriol. 1983; 155:1288–96. [PubMed: 6309747]
107. Grubmeyer C, Skiadopoulos M, Senior AE. L-histidinol dehydrogenase, a Zn2+-metalloenzyme. Arch Biochem Biophys. 1989; 272:311–7. [PubMed: 2665648]
108. Grubmeyer C, Teng H. Mechanism of *Salmonella typhimurium* histidinol dehydrogenase: kinetic isotope effects and pH profiles. Biochemistry. 1999; 38:7355–62. [PubMed: 10353847]
109. Grubmeyer CT, Gray WR. A cysteine residue (cysteine-116) in the histidinol binding site of histidinol dehydrogenase. Biochemistry. 1986; 25:4778–84. [PubMed: 3533140]
110. Guth EC, Francklyn CS. Kinetic discrimination of tRNA identity by the conserved motif 2 loop of a class II aminoacyl-tRNA synthetase. Mol Cell. 2007; 25:531–42. [PubMed: 17317626]
111. Haruyama K, Nakai T, Miyahara I, Hirotsu K, Mizuguchi H, Hayashi H, Kagamiyama H. Structures of *Escherichia coli* histidinol-phosphate aminotransferase and its complexes with histidinol-phosphate and N-(5′-phosphopyridoxyl)-L-glutamate: double substrate recognition of the enzyme. Biochemistry. 2001; 40:4633–44. [PubMed: 11294630]
112. Henderson GB, Snell EE. Crystalline L-histidinol phosphate aminotransferase from *Salmonella typhimurium*. Purification and subunit structure. J Biol Chem. 1973; 248:1906–11. [PubMed: 4632247]

113. Henn-Sax M, Thoma R, Schmidt S, Hennig M, Kirschner K, Sterner R. Two (betaalpha)(8)-barrel enzymes of histidine and tryptophan biosynthesis have similar reaction mechanisms and common strategies for protecting their labile substrates. Biochemistry. 2002; 41:12032–42. [PubMed: 12356303]

114. Henry CS, Jankowski MD, Broadbelt LJ, Hatzimanikatis V. Genome-scale thermodynamic analysis of *Escherichia coli* metabolism. Biophys J. 2006; 90:1453–61. [PubMed: 16299075]

115. Henry T, Garcia-Del Portillo F, Gorvel JP. Identification of *Salmonella* functions critical for bacterial cell division within eukaryotic cells. Mol Microbiol. 2005; 56:252–67. [PubMed: 15773994]

116. Hidalgo M, Rodriguez G, Kuhn JG, Brown T, Weiss G, MacGovren JP, Von Hoff DD, Rowinsky EK. A Phase I and pharmacological study of the glutamine antagonist acivicin with the amino acid solution aminosyn in patients with advanced solid malignancies. Clin Cancer Res. 1998; 4:2763–70. [PubMed: 9829740]

117. Higgins CF, Ames GF, Barnes WM, Clement JM, Hofnung M. A novel intercistronic regulatory element of prokaryotic operons. Nature. 1982; 298:760–2. [PubMed: 7110312]

118. Himeno H, Hasegawa T, Ueda T, Watanabe K, Miura K, Shimizu M. Role of the extra G-C pair at the end of the acceptor stem of tRNA(His) in aminoacylation. Nucleic Acids Res. 1989; 17:7855–63. [PubMed: 2678006]

119. Hoppe I, Johnston HM, Biek D, Roth JR. A refined map of the *hisG* gene of *Salmonella typhimurium*. Genetics. 1979; 92:17–26. [PubMed: 387517]

120. Hsu LC, Okamoto M, Snell EE. L-Histidinol phosphate aminotransferase from *Salmonella typhimurium*. Kinetic behavior and sequence at the pyridoxal-P binding site. Biochimie. 1989; 71:477–89. [PubMed: 2503052]

121. Hsu LM, Klee HJ, Zagorski J, Fournier MJ. Structure of an *Escherichia coli* tRNA operon containing linked genes for arginine, histidine, leucine, and proline tRNAs. J Bacteriol. 1984; 158:934–42. [PubMed: 6327651]

122. Huang L, Pookanjanatavip M, Gu X, Santi DV. A conserved aspartate of tRNA pseudouridine synthase is essential for activity and a probable nucleophilic catalyst. Biochemistry. 1998; 37:344–51. [PubMed: 9425056]

123. Hulton CS, Higgins CF, Sharp PM. ERIC sequences: a novel family of repetitive elements in the genomes of *Escherichia coli*, *Salmonella typhimurium* and other enterobacteria. Mol Microbiol. 1991; 5:825–34. [PubMed: 1713281]

124. Hur S, Stroud RM. How U38, 39, and 40 of many tRNAs become the targets for pseudouridylation by TruA. Mol Cell. 2007; 26:189–203. [PubMed: 17466622]

125. Johnson MS, Taylor BL. Comparison of methods for specific depletion of ATP in *Salmonella typhimurium*. Appl Environ Microbiol. 1993; 59:3509–12. [PubMed: 8250574]

126. Johnston HM, Barnes WM, Chumley FG, Bossi L, Roth JR. Model for regulation of the histidine operon of *Salmonella*. Proc Natl Acad Sci USA. 1980; 77:508–12. [PubMed: 6987654]

127. Johnston HM, Roth JR. DNA sequence changes of mutations altering attenuation control of the histidine operon of *Salmonella typhimurium*. J Mol Biol. 1981; 145:735–56. [PubMed: 6167727]

128. Johnston HM, Roth JR. Histidine mutants requiring adenine: selection of mutants with reduced hisG expression in *Salmonella typhimurium*. Genetics. 1979; 92:1–15. [PubMed: 387516]

129. Jurgens C, Strom A, Wegener D, Hettwer S, Wilmanns M, Sterner R. Directed evolution of a (beta alpha)8-barrel enzyme to catalyze related reactions in two different metabolic pathways. Proc Natl Acad Sci USA. 2000; 97:9925–30. [PubMed: 10944186]

130. Kalousek F, Konigsberg WH. Purification and characterization of histidyl transfer ribonucleic acid synthetase of *Escherichia coli*. Biochemistry. 1974; 13:999–1006. [PubMed: 4591623]

131. Kammen HO, Marvel CC, Hardy L, Penhoet EE. Purification, structure, and properties of *Escherichia coli* tRNA pseudouridine synthase I. J Biol Chem. 1988; 263:2255–63. [PubMed: 3276686]

132. Kasai T. Regulation of the expression of the histidine operon in *Salmonella typhimurium*. Nature. 1974; 249:523–7. [PubMed: 4599761]

133. Kitchingman GR, Fournier MJ. Modification-deficient transfer ribonucleic acids from relaxed control *Escherichia coli*: structures of the major undermodified phenylalanine and leucine

transfer RNAs produced during leucine starvation. Biochemistry. 1977; 16:2213–20. [PubMed: 324516]

134. Kleeman J, Parsons SM. A sensitive assay for the reverse reaction of the first histidine biosynthetic enzyme. Anal Biochem. 1975; 68:236–41. [PubMed: 1190438]
135. Kleeman JE, Parsons SM. Inhibition of histidyl-tRNA-adenosine triphosphate phosphoribosyltransferase complex formation by histidine and by guanosine tetraphosphate. Proc Natl Acad Sci USA. 1977; 74:1535–7. [PubMed: 323857]
136. Klem TJ, Chen Y, Davisson VJ. Subunit interactions and glutamine utilization by *Escherichia coli* imidazole glycerol phosphate synthase. J Bacteriol. 2001; 183:989–96. [PubMed: 11208798]
137. Klem TJ, Davisson VJ. Imidazole glycerol phosphate synthase: the glutamine amidotransferase in histidine biosynthesis. Biochemistry. 1993; 32:5177–86. [PubMed: 8494895]
138. Klungsoyr L, Hagemen JH, Fall L, Atkinson DE. Interaction between energy charge and product feedback in the regulation of biosynthetic enzymes. Aspartokinase, phosphoribosyladenosine triphosphate synthetase, and phosphoribosyl pyrophosphate synthetase. Biochemistry. 1968; 7:4035–40. [PubMed: 4881060]
139. Kronenberg HM, Vogel T, Goldberger RF. A new and highly sensitive assay for the ATP phosphoribosyltransferase that catalyzes the first step of histidine biosynthesis. Anal Biochem. 1975; 65:380–8. [PubMed: 165751]
140. Kryvi H. Thermal stability of phosphoribosyladenosine triphosphate synthetase as reflected in its circular dichroism and activity properties. Effect of inhibitors. Biochim Biophys Acta. 1973; 317:123–30. [PubMed: 4579234]
141. Landick R. The regulatory roles and mechanism of transcriptional pausing. Biochem Soc Trans. 2006; 34:1062–6. [PubMed: 17073751]
142. Lang D, Thoma R, Henn-Sax M, Sterner R, Wilmanns M. Structural evidence for evolution of the beta/alpha barrel scaffold by gene duplication and fusion. Science. 2000; 289:1546–50. [PubMed: 10968789]
143. Lee DN, Landick R. Structure of RNA and DNA chains in paused transcription complexes containing *Escherichia coli* RNA polymerase. J Mol Biol. 1992; 228:759–77. [PubMed: 1281887]
144. Lee F, Yanofsky C. Transcription termination at the trp operon attenuators of *Escherichia coli* and *Salmonella typhimurium*: RNA secondary structure and regulation of termination. Proc Natl Acad Sci USA. 1977; 74:4365–9. [PubMed: 337297]
145. Leopoldseder S, Claren J, Jurgens C, Sterner R. Interconverting the catalytic activities of (betaalpha)(8)-barrel enzymes from different metabolic pathways: sequence requirements and molecular analysis. J Mol Biol. 2004; 337:871–9. [PubMed: 15033357]
146. Lewis JA, Ames BN. Histidine regulation in *Salmonella typhimurium*. XI. The percentage of transfer RNA His charged *in vivo* and its relation to the repression of the histidine operon. J Mol Biol. 1972; 66:131–42. [PubMed: 4339187]
147. Li Y, Altman S. A specific endoribonuclease, RNase P, affects gene expression of polycistronic operon mRNAs. Proc Natl Acad Sci USA. 2003; 100:13213–8. [PubMed: 14585931]
148. Limauro D, Avitabile A, Puglia AM, Bruni CB. Further characterization of the histidine gene cluster of Streptomyces coelicolor A3(2): nucleotide sequence and transcriptional analysis of *hisD*. Res Microbiol. 1992; 143:683–93. [PubMed: 1488552]
149. Liu CE, Ames GF. Characterization of transport through the periplasmic histidine permease using proteoliposomes reconstituted by dialysis. J Biol Chem. 1997; 272:859–66. [PubMed: 8995374]
150. Lohkamp B, McDermott G, Campbell SA, Coggins JR, Lapthorn AJ. The structure of *Escherichia coli* ATP-phosphoribosyltransferase: identification of substrate binding sites and mode of AMP inhibition. J Mol Biol. 2004; 336:131–44. [PubMed: 14741209]
151. Loper JC, Adams E. Purification and Properties of Histidinol Dehydrogenase from *Salmonella typhimurium*. J Biol Chem. 1965; 240:788–95. [PubMed: 14275136]
152. Martin RG. The first enzyme in histidine biosynthesis: the nature of feedback inhibition by histidine. The Journal of Biological Chemistry. 1963; 238:257–268.
153. Martin RG. Presented at the Cold Spring Harbor Symp. Quant. Biol. 1963

154. Martin RG, Berberich B, Ames BN, Davis WW, Goldberger RF, Yourno JD. Enzymes and intermediates of histidine biosynthesis in *Salmonella typhimurium*. Methods Enzymol. 1971; 17B:3–44.

155. Marvel CC, Arps PJ, Rubin BC, Kammen HO, Penhoet EE, Winkler ME. *hisT* is part of a multigene operon in *Escherichia coli* K-12. J Bacteriol. 1985; 161:60–71. [PubMed: 2981810]

156. McGinnis E, Williams LS. Regulation of histidyl-transfer ribonucleic acid synthetase formation in a histidyl-transfer ribonucleic acid synthetase mutant of *Salmonella typhimurium*. J Bacteriol. 1972; 111:739–44. [PubMed: 4559825]

157. Meyers M, Levinthal M, Goldberger RF. trans-Recessive mutation in the first structural gene of the histidine operon that results in constitutive expression of the operon. J Bacteriol. 1975; 124:1227–35. [PubMed: 1104579]

158. Mizuguchi H, Hayashi H, Miyahara I, Hirotsu K, Kagamiyama H. Characterization of histidinol phosphate aminotransferase from *Escherichia coli*. Biochim Biophys Acta. 2003; 1647:321–4. [PubMed: 12686152]

159. Morton DP, Parsons SM. Biosynthetic direction substrate kinetics and product inhibition studies on the first enzyme of histidine biosynthesis, adenosine triphosphate phosphoribosyltransferase. Arch Biochem Biophys. 175:677–86. [PubMed: 183121]

160. Morton DP, Parsons SM. Inhibition of ATP phosphoribosyltransferase by AMP and ADP in the absence and presence of histidine. Arch Biochem Biophys. 1977; 181:643–8. [PubMed: 332083]

161. Morton DP, Parsons SM. Synergistic inhibition of ATP phosphoribosyltransferase by guanosine tetraphosphate and histidine. Biochem Biophys Res Commun. 1977; 74:172–7. [PubMed: 319792]

162. Muralla R, Sweeney C, Stepansky A, Leustek T, Meinke D. Genetic dissection of histidine biosynthesis in Arabidopsis. Plant Physiol. 2007; 144:890–903. [PubMed: 17434988]

163. Murray ML, Hartman PE. Overproduction of *hisH* and *hisF* gene products leads to inhibition of cell cell division in *Salmonella*. Can J Microbiol. 1972; 18:671–81. [PubMed: 4557275]

164. Myers RS, Amaro RE, Luthey-Schulten ZA, Davisson VJ. Reaction coupling through interdomain contacts in imidazole glycerol phosphate synthase. Biochemistry. 2005; 44:11974–85. [PubMed: 16142895]

165. Myers RS, Jensen JR, Deras IL, Smith JL, Davisson VJ. Substrate-induced changes in the ammonia channel for imidazole glycerol phosphate synthase. Biochemistry. 2003; 42:7013–22. [PubMed: 12795596]

166. Nagai A, Ward E, Beck J, Tada S, Chang JY, Scheidegger A, Ryals J. Structural and functional conservation of histidinol dehydrogenase between plants and microbes. Proc Natl Acad Sci USA. 1991; 88:4133–7. [PubMed: 2034659]

167. Neidhardt, FC. Chemical composition of *Escherichia coli*.. In: Neidhardt, FC.; Ingraham, JL.; Low, KB.; Magasanik, B.; Schaechter, M.; Umbarger, HE., editors. *Escherichia coli* and *Salmonella typhimurium*: Cellular and Molecular Biology.. American Society for Microbiology; Washington, DC.: 1987.

168. Nikaido K, Liu PQ, Ames GF. Purification and characterization of HisP, the ATP-binding subunit of a traffic ATPase (ABC transporter), the histidine permease of Salmonella typhimurium. Solubility, dimerization, and ATPase activity. J Biol Chem. 1997; 272:27745–52. [PubMed: 9346917]

169. O'Byrne CP, Ni Bhriain N, Dorman CJ. The DNA supercoiling-sensitive expression of the *Salmonella typhimurium* his operon requires the his attenuator and is modulated by anaerobiosis and by osmolarity. Mol Microbiol. 1992; 6:2467–76. [PubMed: 1406284]

170. O'Donovan GA, Ingraham JL. Cold-sensitive mutants of *Escherichia coli* resulting from increased feedback inhibition. Proc Natl Acad Sci USA. 1965; 54:451–7. [PubMed: 5324392]

171. Ohashi Y, Hirayama A, Ishikawa T, Nakamura S, Shimizu K, Ueno Y, Tomita M, Soga T. Depiction of metabolome changes in histidine-starved *Escherichia coli* by CE-TOFMS. Mol Biosyst. 2008; 4:135–47. [PubMed: 18213407]

172. Ow MC, Kushner SR. Initiation of tRNA maturation by RNase E is essential for cell viability in E. coli. Genes Dev. 2002; 16:1102–15. [PubMed: 12000793]

173. Palmer DT, Blum PH, Artz SW. Effects of the hisT mutation of *Salmonella typhimurium* on translation elongation rate. J Bacteriol. 1983; 153:357–63. [PubMed: 6401282]
174. Parsons SM, Koshland DE Jr. A rapid isolation of phosphoribosyladenosine triphosphate synthetase and comparison to native enzyme. J Biol Chem. 1974; 249:4104–9. [PubMed: 4368347]
175. Paul BJ, Berkmen MB, Gourse RL. DksA potentiates direct activation of amino acid promoters by ppGpp. Proc Natl Acad Sci USA. 2005; 102:7823–8. [PubMed: 15899978]
176. Pease AJ, Roa BR, Luo W, Winkler ME. Positive growth rate-dependent regulation of the *pdxA*, *ksgA*, and *pdxB* genes of *Escherichia coli* K-12. J Bacteriol. 2002; 184:1359–69. [PubMed: 11844765]
177. Piszkiewicz D, Tilley BE, Rand-Meir T, Parsons SM. Amino acid sequence of ATP phosphoribosyltransferase of *Salmonella typhimurium*. Proc Natl Acad Sci USA. 1979; 76:1589–92. [PubMed: 377278]
178. Pons FW, Neubert U, Muller P. Evidence for frameshift mutations in the hisH gene of *Escherichia coli* causing synthesis of a partially active glutamine amidotransferase. Genetics. 1988; 120:657–65. [PubMed: 3066682]
179. Price MN, Alm EJ, Arkin AP. The histidine operon is ancient. J Mol Evol. 2006; 62:807–8. [PubMed: 16612542]
180. Prival MJ, Cebula TA. Sequence analysis of mutations arising during prolonged starvation of *Salmonella typhimurium*. Genetics. 1992; 132:303–10. [PubMed: 1427030]
181. Rangarajan ES, Proteau A, Wagner J, Hung MN, Matte A, Cygler M. Structural snapshots of *Escherichia coli* histidinol phosphate phosphatase along the reaction pathway. J Biol Chem. 2006; 281:37930–41. [PubMed: 16966333]
182. Riccio A, Bruni CB, Rosenberg M, Gottesman M, McKenney K, Blasi F. Regulation of single and multicopy his operons in *Escherichia coli*. J Bacteriol. 1985; 163:1172–9. [PubMed: 2993236]
183. Riggs D, Artz S. The *hisD-hisC* gene border of the *Salmonella typhimurium* histidine operon. Mol Gen Genet. 1984; 196:526–9. [PubMed: 6390096]
184. Riggs DL, Mueller RD, Kwan HS, Artz SW. Promoter domain mediates guanosine tetraphosphate activation of the histidine operon. Proc Natl Acad Sci USA. 1986; 83:9333–7. [PubMed: 3540936]
185. Roth JR, Anton DN, Hartman PE. Histidine regulatory mutants in *Salmonella typhimurium*. I. Isolation and general properties. J Mol Biol. 1966; 22:305–23. [PubMed: 5339687]
186. Rudd KE, Bochner BR, Cashel M, Roth JR. Mutations in the *spoT* gene of *Salmonella typhimurium*: effects on *his* operon expression. J Bacteriol. 1985; 163:534–42. [PubMed: 3894329]
187. Rudd KE, Menzel R. *his* operons of *Escherichia coli* and *Salmonella typhimurium* are regulated by DNA supercoiling. Proc Natl Acad Sci USA. 1987; 84:517–21. [PubMed: 3025879]
188. Schimmel P, Giege R, Moras D, Yokoyama S. An operational RNA code for amino acids and possible relationship to genetic code. Proc Natl Acad Sci USA. 1993; 90:8763–8. [PubMed: 7692438]
189. Schmid MB, Roth JR. Internal promoters of the his operon in *Salmonella typhimurium*. J Bacteriol. 1983; 153:1114–9. [PubMed: 6296044]
190. Schramm G, Zapatka M, Eils R, Konig R. Using gene expression data and network topology to detect substantial pathways, clusters and switches during oxygen deprivation of *Escherichia coli*. BMC Bioinformatics. 2007; 8:149. [PubMed: 17488495]
191. Schweitzer BA, Loida PJ, CaJacob CA, Chott RC, Collantes EM, Hegde SG, Mosier PD, Profeta S. Discovery of imidazole glycerol phosphate dehydratase inhibitors through 3-D database searching. Bioorg Med Chem Lett. 2002; 12:1743–6. [PubMed: 12067551]
192. Scott JF, Roth JR, Artz SW. Regulation of histidine operon does not require *hisG* enzyme. Proc Natl Acad Sci USA. 1975; 72:5021–5. [PubMed: 1108009]
193. Shand RF, Blum PH, Mueller RD, Riggs DL, Artz SW. Correlation between histidine operon expression and guanosine 5′-diphosphate-3′-diphosphate levels during amino acid downshift in

stringent and relaxed strains of *Salmonella typhimurium*. J Bacteriol. 1989; 171:737–43. [PubMed: 2492514]

194. Sheppard DE. Mutants of *Salmonella typhimurium* Resistant to Feedback Inhibition by L-Histidine. Genetics. 1964; 50:611–23. [PubMed: 14221869]
195. Shyamala V, Schneider E, Ames GF. Tandem chromosomal duplications: role of REP sequences in the recombination event at the join-point. Embo J. 1990; 9:939–46. [PubMed: 2178927]
196. Singer CE, Smith GR, Cortese R, Ames BN. [Mutant tRNA His ineffective in repression and lacking two pseudouridine modifications.]. Nat New Biol. 1972; 238:72–4. [PubMed: 4558263]
197. Sinha SC, Chaudhuri BN, Burgner JW, Yakovleva G, Davisson VJ, Smith JL. Crystal structure of imidazole glycerol-phosphate dehydratase: duplication of an unusual fold. J Biol Chem. 2004; 279:15491–8. [PubMed: 14724278]
198. Sissler M, Delorme C, Bond J, Ehrlich SD, Renault P, Francklyn C. An aminoacyl-tRNA synthetase paralog with a catalytic role in histidine biosynthesis. Proc Natl Acad Sci USA. 1999; 96:8985–90. [PubMed: 10430882]
199. Sivaraman J, Li Y, Larocque R, Schrag JD, Cygler M, Matte A. Crystal structure of histidinol phosphate aminotransferase (HisC) from *Escherichia coli*, and its covalent complex with pyridoxal-5′-phosphate and lhistidinol phosphate. J Mol Biol. 2001; 311:761–76. [PubMed: 11518529]
200. Sivaraman J, Myers RS, Boju L, Sulea T, Cygler M, Jo Davisson V, Schrag JD. Crystal structure of Methanobacterium thermoautotrophicum phosphoribosyl-AMP cyclohydrolase HisI. Biochemistry. 2005; 44:10071–80. [PubMed: 16042384]
201. Smith DW, Ames BN. Intermediates in the early steps of histidine biosynthesis. J Biol Chem. 1964; 239:1848–55. [PubMed: 14213364]
202. Smulski DR, Huang LL, McCluskey MP, Reeve MJ, Vollmer AC, Van Dyk TK, LaRossa RA. Combined, functional genomic-biochemical approach to intermediary metabolism: interaction of acivicin, a glutamine amidotransferase inhibitor, with *Escherichia coli* K-12. J Bacteriol. 2001; 183:3353–64. [PubMed: 11344143]
203. Sonenshein, AL. Introduction to metabolic pathways. In: Sosenshein, AL.; Hoch, JA.; Losick, R., editors. Bacillus subtilis and Other Gram Positive Bacteria. American Society for Microbiology; Washington, D.C.: 1993. p. 127-132.
204. Stepansky A, Leustek T. Histidine biosynthesis in plants. Amino Acids. 2006; 30:127–42. [PubMed: 16547652]
205. Stephens JC, Artz SW, Ames BN. Guanosine 5′-diphosphate 3′-diphosphate (ppGpp): positive effector for histidine operon transcription and general signal for amino-acid deficiency. Proc Natl Acad Sci U S A. 1975; 72:4389–93. [PubMed: 1105582]
206. Sterboul CC, Kleeman JE, Parsons SM. Purification and characterization of a mutant ATP phosphoribosyltransferase hypersensitive to histidine feedback inhibition. Arch Biochem Biophys. 1977; 181:632–42. [PubMed: 332082]
207. Stern MJ, Ames GF, Smith NH, Robinson EC, Higgins CF. Repetitive extragenic palindromic sequences: a major component of the bacterial genome. Cell. 1984; 37:1015–26. [PubMed: 6378385]
208. Tebar AR, Ballesteros AO. Kinetic properties of ATP phosphoribosyltransferase of *Escherichia coli*. Mol Cell Biochem. 1976; 11:131–6. [PubMed: 781521]
209. Tebar AR, Fernandez VM, Martin Del Rio R, Ballesteros AO. Studies on the quaternary structure of the first enzyme for histidine biosynthesis. Experientia. 1973; 29:1477–9. [PubMed: 4358959]
210. Teng H, Grubmeyer C. Mutagenesis of histidinol dehydrogenase reveals roles for conserved histidine residues. Biochemistry. 1999; 38:7363–71. [PubMed: 10353848]
211. Teng H, Segura E, Grubmeyer C. Conserved cysteine residues of histidinol dehydrogenase are not involved in catalysis. Novel chemistry required for enzymatic aldehyde oxidation. J Biol Chem. 1993; 268:14182–8. [PubMed: 8314784]
212. Thomale J, Nass G. Alteration of the intracellular concentration of aminoacyl-tRNA synthetases and isoaccepting tRNAs during amino-acid limited growth in *Escherichia coli*. Eur J Biochem. 1978; 85:407–18. [PubMed: 348470]

213. Toone WM, Rudd KE, Friesen JD. deaD, a new *Escherichia coli* gene encoding a presumed ATP-dependent RNA helicase, can suppress a mutation in *rpsB*, the gene encoding ribosomal protein S2. J Bacteriol. 1991; 173:3291–302. [PubMed: 2045359]

214. Toulokhonov I, Zhang J, Palangat M, Landick R. A central role of the RNA polymerase trigger loop in active-site rearrangement during transcriptional pausing. Mol Cell. 2007; 27:406–19. [PubMed: 17679091]

215. Tsui HC, Arps PJ, Connolly DM, Winkler ME. Absence of hisT-mediated tRNA pseudouridylation results in a uracil requirement that interferes with *Escherichia coli* K-12 cell division. J Bacteriol. 1991; 173:7395–400. [PubMed: 1938930]

216. Turnbough CL Jr. Neill RJ, Landsberg R, Ames BN. Pseudouridylation of tRNAs and its role in regulation in *Salmonella typhimurium*. J Biol Chem. 1979; 254:5111–9. [PubMed: 376505]

217. Urbonavicius J, Qian Q, Durand JM, Hagervall TG, Bjork GR. Improvement of reading frame maintenance is a common function for several tRNA modifications. Embo J. 2001; 20:4863–73. [PubMed: 11532950]

218. Verde P, Frunzio R, di Nocera PP, Blasi F, Bruni CB. Identification, nucleotide sequence and expression of the regulatory region of the histidine operon of *Escherichia coli* K-12. Nucleic Acids Res. 1981; 9:2075–86. [PubMed: 6170941]

219. Vitreschak AG, Lyubetskaya EV, Shirshin MA, Gelfand MS, Lyubetsky VA. Attenuation regulation of amino acid biosynthetic operons in proteobacteria: comparative genomics analysis. FEMS Microbiol Lett. 2004; 234:357–70. [PubMed: 15135544]

220. Vrentas CE, Gaal T, Ross W, Ebright RH, Gourse RL. Response of RNA polymerase to ppGpp: requirement for the omega subunit and relief of this requirement by DksA. Genes Dev. 2005; 19:2378–87. [PubMed: 16204187]

221. Whitfield HJ Jr. Gutnick DL, Margolies MN, Martin RG, Rechler MM, Voll MJ. Relative translation frequencies of the cistrons of the histidine operon. J Mol Biol. 1970; 49:245–9. [PubMed: 4915861]

222. Winkler ME, Roth DJ, Hartman PE. Promoter- and attenuator-related metabolic regulation of the *Salmonella typhimurium* histidine operon. J Bacteriol. 1978; 133:830–43. [PubMed: 342509]

223. Winkler ME, Zawodny RV, Hartman PE. Mutation *spoT* of *Escherichia coli* increases expression of the histidine operon deleted for the attenuator. J Bacteriol. 1979; 139:993–1000. [PubMed: 383702]

224. Xiao H, Kalman M, Ikehara K, Zemel S, Glaser G, Cashel M. Residual guanosine 3′,5′-bispyrophosphate synthetic activity of relA null mutants can be eliminated by *spoT* null mutations. J Biol Chem. 1991; 266:5980–90. [PubMed: 2005134]

225. Yanofsky C, Platt T, Crawford IP, Nichols BP, Christie GE, Horowitz H, VanCleemput M, Wu AM. The complete nucleotide sequence of the tryptophan operon of *Escherichia coli*. Nucleic Acids Res. 1981; 9:6647–68. [PubMed: 7038627]

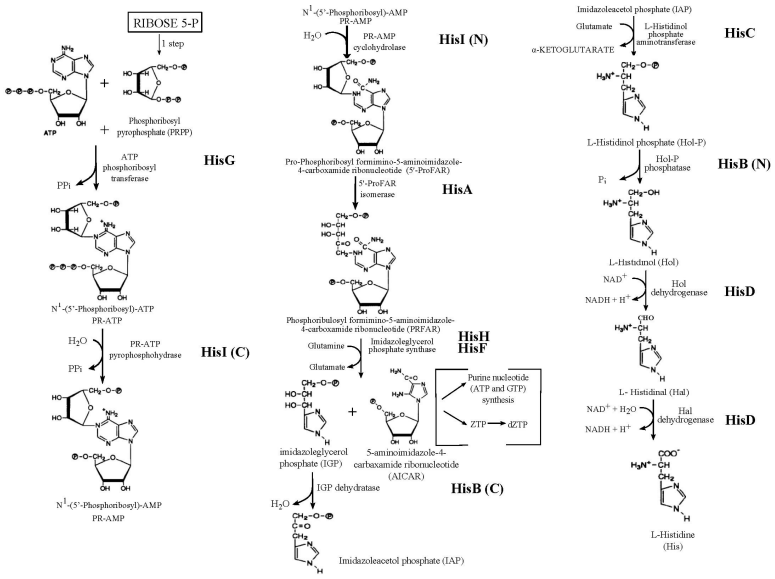

FIGURE 1.

Histidine biosynthetic pathway. The steps in the pathway are described in the text, and the enzymes that catalyze the reactions are listed in Table 1. When the enzymes are bifunctional (C) indicates that the carboxyl terminal is performing the reaction and (N) indicates that the amino terminal is performing the reaction.

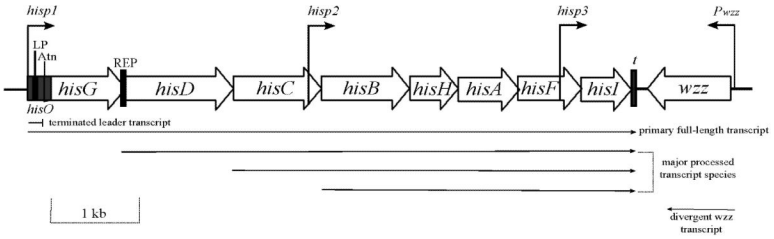

FIGURE 2.

Diagram of the *his* operon in *E. coli* and *S. typhimurium* drawn to scale. *hisp1*, *his* operon primary promoter; LP, leader peptide; *Atn*, *his* attenuator; *hisp2* and *hisp3*, *his* operon internal promoters; *t*, terminator at the end of operon; REP is a repetitive extragenic palindromic element that is present between *hisG* and *hisD* in *S. typhimurium* but not in *E. coli*; *Pwzz*, promoter of *wzz* gene. Arrows at the bottom of the figure show the length of the transcripts.

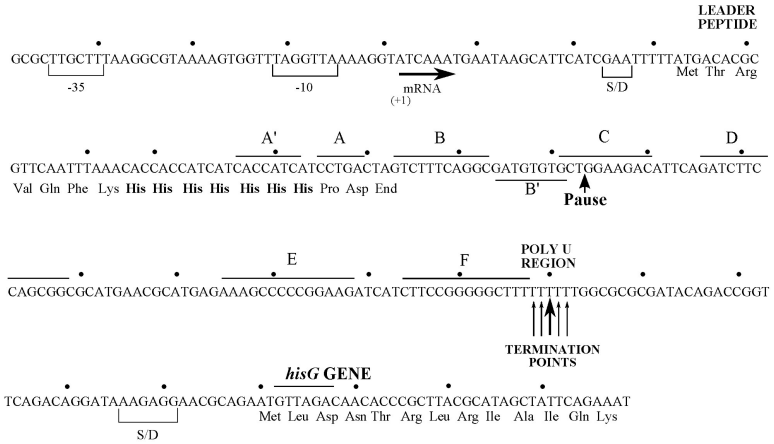

FIGURE 3.

DNA sequence of the *hisO* region in *S. typhimurium*. The -35 and -10 regions of the *hisp1* promoter and the start point of transcription are indicated. S/D designates the weak and strong Shine-Dalgarno sequences in the translation initiation regions for the *his* leader peptide and *hisG* polypeptide, respectively. A′, A, B, B′, C, D, E, and F refer to segments of the *his* leader transcript that can base pair to form the alternative, mutually exclusive RNA secondary structures shown in Fig. 4. The site of pausing by RNA polymerase during *in vitro* transcription of the *his* leader region is indicated (59). The major (heavy arrow) and minor (light arrows) are points of transcription termination in the *his* attenuator region. Figure is redrawn from reference (25).

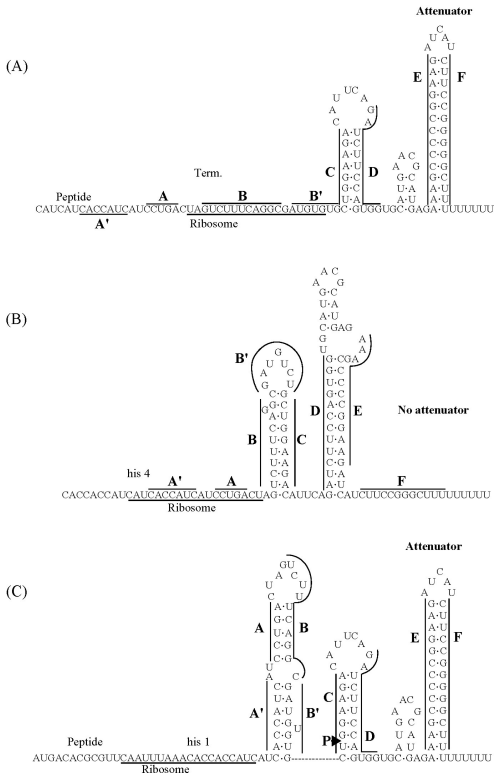

FIGURE 4.

Mutually exclusive, alternative stem-and-loop structures that form in the *his* leader transcript as part of the attenuation process. Letters designate segments of the leader transcript that base pair to form secondary structures. Ribosomes labeled lines indicate the nucleotides masked by a ribosome stopped at a codon. The model for *his* attenuation is described in the text. (A) Transcription termination configuration caused by translation of the leader transcript to the UAG stop codon; (B) readthrough transcription configuration caused by ribosome stalling at the fourth histidine codon in the leader transcript; (C) transcription termination configuration caused by ribosome stalling at the Gln codon in the leader transcript. Configuration C will also occur in the absence of translation of the leader transcript or after rapid dissociation of the ribosome at the translation stop codon. Configuration C also indicates the pause site (arrowhead marked with P) where RNA polymerase temporarily halts elongation following synthesis of A:B (57, 59, 146). The role of pausing in synchronizing the attenuation mechanism is described in the text. Figure modified from reference (127).

TABLE 1

Properties of enzymes encoded by the *his* operon and major *his* regulatory loci

Enzyme	**Gene**	**Mol wt of monomer[a] (# amino acids)**	**Association state of enzyme[b] and references for crystal structures[c]**	**Kinetic parameters of enzymes from *E. coli* and *S. typhimurium*[d]**	**Inhibitors**	**References for kinetic parameters and, inhibitors**
ATP phosphoribosyltransferase (EC 2.4.2.17)	*hisG*	33,271 (299)	Dimer when PRPP and ATP bound (active state); hexamer; when histidine and AMP bound (inhibited state)	K_m (apparent) (ATP) = 70-110μM; K_m(apparent) (PRPP) = 11-30 μM; K_m (conc. independent) (ATP) =800 μM; K_m (conc. independent) (PRPP) =110 μM; ping-pong bi-bi mechanism	Histidine (K_i = 60-380 μM); 2-thiazole-alanine; AMP (K_i [apparent] = 860 μM); ADP; AMP + histidine > AMP; ppGpp + histidine >histidine; PR-ATP (product)	(42, 71, 159-161, 206, 208)
Histidinol dehydrogenase (EC 1.1.1.23)	*hisD* (bi-functional)	46,113 (432)	Dimer with 2 Zn^{2+}	K_m (NAD^+) = 600-1,300 μM; K_m (Hol) =11-18 μM; K_d (Zn^{2+}) = 50 μM; acid-base catalysis	Histamine (K_i = 40 μM); imidazole (K_i = 1.5 mM)	(109, 151, 210, 211)
Histidinol phosphate aminotransferase (EC 2.6.1.9)	*hisC*	39,319 (356)	Dimer	K_m (IAP) = 80-120 μM; K_m (glutamate) = 7 mM; ping-pong bi-bi mechanism	Hol-P (product; K_i = 52-160 μM); IAP (substrate; K_i = 0.9 mM); various substrate analogs	(1, 120)
IGP dehydratase (C-terminal domain) (EC 4.2.1.19): histidinol phosphatase (N-terminal domain) (EC 3.1.3.15)	*hisB* (bi-functional)	40,283 (352)	24-mer in the presence of Mn^{+2}; Hol Pase binds Zn^{+2}	K_m (IPG) = 700 μM; K_m (Hol-P) = 300 μM; HisB-N (Hol-P) = 54 μM and $k_{cat} = 2 \times 10^3$ s^{-1}	3-Amino-1,2,4-triazole and herbicides inhibit dehydratase; Ca^{+2} inhibits Hol Pase	(41, 103, 181, 191)
IGP synthase subunit (glutaminase)	*hisH*	21,655 (196)	Heterodimer with HisF (see below)	IGP synthase: K_m^{app} (glutamine) = 240 μM; K_m^{app} (PRFAR) = 1.5 μM; $k_{cat} \approx 9$ s^{-1}	Acivicin; K_i^{app} = 1.5 μM	(64, 137, 202)
Phosphoribosylformimino-5-amino-1-phosphoribosyl -4-imidazole carboxamide isomerase (EC 5.3.1.16)	*hisA*	26,035 (245)	Monomer	At 25° C, K_m (ProFAR) = 1.6 μM and k_{cat} = 4.9 s^{-1}; at 37° C, K_m (ProFAR) = 1.8 μM and k_{cat} = 14.3 s^{-1};	Unknown	(113)
IGP synthase subunit (cyclo-ligase)	*hisF*	28, 457 (258)	Heterodimer with HisH (see above)	Cyclo-ligase in absence of HisH subunit; K_m (PRFAR) = 21 μM; K_m (NH_4Cl) = 266 mM	Unknown	(137)
Phosphoribosyl-ATP pyrophosphohydrolase (“HisE” activity in C-terminal domain); phosphoribosyl-AMP cyclohydrolase (“HisI” activity in N-terminal domain) (EC 3.5.4.19)	*hisI* (bifunctional; formerly *hisIE*)	22,764 (203)	Dimer; HisI binds Zn^{+2} and requires Mg^{+2}	Pyrophosphohydrolase (HisE) remains unknown; cyclohydrolase (HisI) of *M. vannielii* K_m (PR-AMP) = 9.9; k_{cat} = 4.1 s^{-1}	EDTA	(69)
Histidyl-tRNA synthetase (EC 6.1.1.21)	*hisS*	46,898 (424)	Dimer	Aminoacylation: K_m (His) = 3.2-25 μM; K_m(ATP) = 140 μM; K_m ($tRNA^{His}$) = 0.04 –	α-Methylhistidine; histidinol; adenosine;	(42-44, 46, 96, 97, 130)

Enzyme	Gene	Mol wt of monomer[a] (# amino acids)	Association state of enzyme[b] and references for crystal structures[c]	Kinetic parameters of enzymes from *E. coli* and *S. typhimurium*[d]	Inhibitors	References for kinetic parameters and, inhibitors
				1.5 μM; K_{cat}^{app} = 3 $s^{=1}$; pyrophosphate exchange: ATP ; pyrophosphate exchange: K_m^{app}(His) = 87 μM; k_{cat}^{app} (His) = 91 s^{-1}; K_m^{app}(ATP) = 641 μM; k_{cat}^{app} (ATP) = 170 s^{-1}	AMP; ADP; AMP + PP_i > AMP; His-$tRNA^{His}$ (product)	
Pseudouridine synthase I	*truA* (*hisT*)	30,399 (270)	Dimer	K_m (tRNA) 1.8 μM and K_{cat} = 0.2 s^{-1} at 15°C		(68, 122)

[a] Polypeptide molecular weights are from the following sources: *E.coli* his operon DNA sequence (49) *E.coli* his DNA sequence (99); *E.coli hisT* DNA sequence (21).

[b] Enzyme native molecular weights are from the following sources: HisG (34, 208); HisD (34, 107, 211); HisC (34, 112, 120); HisB (181), HisH-HisF (137); HisA (113, 142); HisI (69); HisRS (20, 74, 130); TruA (HisT) (94).

[c] Crystal structures can be found in the following references. Some structures are from thermophilic species or fungi, rather than *E. coli* and *S. typhimurium*. HisG (56, 65, 150); HisD (26); HisC (111, 199); HisB (181, 197); HisH-HisF (11, 61, 80, 165); HisA (113, 142); HisI (200); HisRS (19, 20, 96, 110); TruA (HisT) (94, 124).

[d] Enzyme assay protocols can be found in the references. Additional and updated assay methods can be found in the following references: all of the *his* operon encoded enzymes (154), HisG (134, 139, 208); HisD (67, 107, 213); HisC (120); HisB (phosphatase activity) (40, 83); HisS (76, 92, 97); HisT (68, 155). Full substrate names and structures corresponding to abbreviations are given in Fig. 1.

TABLE 2

Parameters of histidine biosynthesis in wild-type *S. typhimurium* and *E. coli*

Parameter[a]	**Growth condition**[b]	**Value**	**References**
Intracellular free His concn	Minimal medium	15 μM	(17)
	Minimal medium + 50 μM His	100 μM	
Total residue composition of His in protoplasm	Minimal medium	90 μmol/g of dried cells	(167)
% of RNA^{His} charged with His	Minimal medium	77%	(146)
	Minimal medium + 50 μM His	88%	
Relative *his* operon expression	Minimal medium	≡1.0	(42, 222)
	Minimal medium + 50 μM His	0.9	
	Rich medium	0.3	
Steady-state rate of His biosynthesis	Minimal medium	≈ 1 μmol/g (dry wt)/min	(42)

[a] Additional relevant parameters: the K_m for histidine transport is approximately 10^{-8} for the high affinity periplasmic-binding protein (HisJ-HisQ-HisM-HisP) permease (16). The intracellular concentrations of the following compounds were estimated for bacteria growing in minimal-glucose medium: 3,000 μM ATP; 31 μM ppGpp; 2 μM $tRNA^{His}$; 2 μM histidyl-tRNA synthetase (35, 73).

[b] Glucose is the carbon source in the minimal medium. Rich medium is Luria-Bertani (LB) or nutrient broth

TABLE 3

Parameters of the *his* operon structure and regulation

Parameter[a]	**Comments**	**Organism**[b]	**Reference(s)**
Gene order; length	OGDCBHAFI; 7,389 nt OG-(REP[b])-DCBHAFI; 7,438 nt	*E.coli* *S. typhimurium*	(49)
Size of full-length primary transcript: *hisp1* to *t*	7,337 nt (DNA sequence) 7,390 nt (DNA sequence) ≈7,300 (Northern blot)	*E.coli* *S. typhimurium* *E.coli* and *S. typhimurium*	(5, 49)
Primary transcript half-life	≈4 min	*S. typhimurium*	
Sizes of major processed transcripts on Northern blots	≈6,300 (*hisDCBHAFI*) ≈5,000 (*hisCBHAFI*) ≈3,900 (*hisBHAFI*)[c]	*S. typhimurium*	(5)
Size of major terminated leader transcript: *hisp1* to A	180 nt 177 nt	*E.coli* *S. typhimurium*	(49, 59, 99, 100)
Sizes of secondary transcript[d]	*hisp2* to *t* 3,943 nt 3,888 nt *hisp3* to *t* 809 nt 763 nt	*E.coli* *S. typhimurium* *E.coli* *S. typhimurium*	(5, 6, 49)
% of transcripts from *hisp2* relative to *hisp1* in wild-type bacteria	≤10% (and *hisp2* is stronger than *hisp3*)	*S. typhimurium*	(5)
Established modes of operon regulation	ppGpp stimulation of transcription initiation from *hisp1* Attenuation control in response to His-tRNA^{His} concentration, which changes in response to histidine supply and chromosomal DNA supercoiling density (see text)	*E. coli* and *S. typhimurium* (but mainly *S. typhimurium*)	See text
Type of terminator (*t*) at end of operon	Bidirectional, Rho factor independent	*E. coli* and *S. typhimurium*	(31, 52)

[a] *hisp1*, *his* operon primary promoter; A, *his* attenuator; *hisp2* and *hisp3*, *his* operon internal promoters; *t*, terminator at the end of operon (see Fig. 2)

[b] REP is a repetitive extragenic palindromic element that is present between *hisG* and *hisD* in *S. typhimurium* but not in *E. coli* (123, 207).

[c] The half-life of the 3,900-nt *hisBHAFI* transcript is exceptionally long (> >15 min) (5, 49).

[d] Determined from the DNA sequences and by Northern blotting and SI mapping.